

# A market mechanism for multiple air traffic resources

Irene Brugnara<sup>a</sup>, Lorenzo Castelli<sup>a,\*</sup>, Raffaele Pesenti<sup>b</sup>

<sup>a</sup>*Università degli Studi di Trieste, Trieste, Italy*

<sup>b</sup>*Università Ca' Foscari di Venezia, Venezia, Italy*

---

---

## Highlights

- Our model optimises the cost of delay in multiple ATFM regulations while preserving the confidentiality of costs for airlines
- Our market mechanism is individual rational, weakly budget balanced, and allocative efficient
- We apply Lagrangean relaxation and the subgradient method to an integer programming problem
- All numerical experiments are performed on real traffic data

---

\*Corresponding author

*Email address:* [castelli@units.it](mailto:castelli@units.it) (Lorenzo Castelli)

# A market mechanism for multiple air traffic resources

Irene Brugnara<sup>a</sup>, Lorenzo Castelli<sup>a,\*</sup>, Raffaele Pesenti<sup>b</sup>

<sup>a</sup>*Università degli Studi di Trieste, Trieste, Italy*

<sup>b</sup>*Università Ca' Foscari di Venezia, Venezia, Italy*

---

## Abstract

We introduce a model that extends the concept of air traffic flow management slot to the concept of time window, allowing to effectively deal with a network of interacting regulations. The model aims at minimising the total cost of delay of a time window allocation to flights and is based on an integer programming problem. It consists in a market-based mechanism between flights and a central authority to trade time windows, which fulfils the properties of individual rationality (every participating airline has a non-negative profit from the mechanism) and weak budget-balance (the mechanism requires no external subsidisation). Equity is assumed to be respected because the First Planned First Served allocation as an endowment guaranteed to all flights and allocated for free. The proposed market mechanism can be implemented in a distributed manner preventing the disclosure of confidential information by airlines, and is based on the Lagrangian relaxation of the integer optimisation problem, solved through the subgradient algorithm. We present some computational experiments conducted to test the model on some real instances of air traffic data.

*Keywords:* Air Traffic Management (ATM), Air Traffic Flow Management (ATFM), ATFM regulation, subgradient algorithm, market mechanism, pricing equilibrium.

---

---

\*Corresponding author

*Email address:* [castelli@units.it](mailto:castelli@units.it) (Lorenzo Castelli)

# A market mechanism for multiple air traffic resources

---

## Abstract

We introduce a model that extends the concept of air traffic flow management slot to the concept of time window, allowing to effectively deal with a network of interacting regulations. The model aims at minimising the total cost of delay of a time window allocation to flights and is based on an integer programming problem. It consists in a market-based mechanism between flights and a central authority to trade time windows, which fulfils the properties of individual rationality (every participating airline has a non-negative profit from the mechanism) and weak budget-balance (the mechanism requires no external subsidisation). Equity is assumed to be respected because the First Planned First Served allocation is an endowment guaranteed to all flights and allocated for free. The proposed market mechanism can be implemented in a distributed manner preventing the disclosure of confidential information by airlines, and is based on the Lagrangian relaxation of the integer optimisation problem, solved through the subgradient algorithm. We present some computational experiments conducted to test the model on some real instances of air traffic data.

*Keywords:* Air Traffic Management (ATM), Air Traffic Flow Management (ATFM), ATFM regulation, subgradient algorithm, market mechanism, pricing equilibrium.

---

## 1. Introduction

Air traffic resources consisting in airports and airspace volumes have a limited capacity in terms of number of aircraft that can enter the resource in a given period of time. The factor determining capacity is the amount of traffic that can be safely handled by air traffic controllers. In the current European Air Traffic Flow Management (ATFM) system, when an imbalance between traffic demand and available capacity is foreseen in an airport or airspace volume, the Network Manager (NM) can impose an ATFM regulation, which limits the rate of aircraft that can enter the regulated resource in a given period of time. This ATFM measure is achieved by delaying the departure of flights from their origin airport. ATFM delays are imposed to flights through an ATFM slot, a 15-minute tolerance time interval that flights have to comply with for departure. In the current system, ATFM slots are allocated to flights according to a First Planned First Served (FPFS) principle.

Besides a better management of ATC sectors through configurations or splitting of sectors, alternatives to ATFM regulations to resolve congestion are for example re-routing of traffic flows. These choices, however, “have a negative impact on the environment due to longer routes and/or sub-optimal altitude profiles” (Dalmau, 2022). ATFM regulations also have a negative economic impact because ATFM delays represent a cost for airlines: pre-pandemic estimations report 1.93B€ in 2018 and 1.76 B€ in 2019 (Performance Review Commission, 2019). Recently, new quantitative and qualitative indicators to assess the expected impact of the costs ATFM regulations would impose on airspace users have been defined (Delgado et al., 2021). Therefore economic benefits are possible by considering an allocation of ATFM slots that takes into account the different impact that delays have on costs for airlines. Added to these savings are environmental benefits since a possible reduction in costs due to ATFM delays makes the rerouting option less attractive.

The most immediate way to change the FPFS allocation is to let the NM centrally determine an allocation that minimises the overall costs of the delay. However, this solution is not feasible mainly

25 for two reasons: on the one hand, a single airline could eventually have a higher cost of delay with this  
26 new allocation than with FPFS (for the benefit of the system optimum a user is particularly penalised)  
27 and therefore it is not clear why it should agree to deviate from it. On the other hand, airlines need to  
28 communicate their delay costs to the NM and this is sensitive information that is released very reluctantly.  
29 It is therefore necessary to identify mechanisms which in some way involve airlines or which at least do  
30 not oblige them to disclose confidential information.

31 Since for each regulation the number of slots is fixed (see Section 3.1), modifying the FPFS allocation  
32 means in practice allowing an exchange of slots (which we also refer to as slot *trade* or *swap*). In  
33 the United States context, Vossen and Ball (2006a,b) and Sherali et al. (2011) propose mathematical  
34 programming models for the exchange between airlines (inter-airlines) of slots if some flights are cancelled  
35 or further delayed compared to the initial allocation. Delays are assigned within a *Ground delay program*  
36 (Liu et al., 2019) where the ration by schedule (RBS) procedure is used to allocate slots (RBS follows  
37 the same principles of the FPFS). These models require trading to be regulated by a “mediator” (the  
38 FAA in their case), but they do not involve monetary aspects. However, the possibility of designing  
39 “market-based mechanisms in which airlines would be able to buy and sell slots” is mentioned since  
40 “benefits could be substantial” (Vossen and Ball, 2006b). This suggestion was taken in by Castelli et al.  
41 (2011b) who developed a market mechanism that enables airlines to pay for delay reduction or receive  
42 compensation for delay increase by adapting the Vossen and Ball (2006a) model to the European context.  
43 This mechanism fulfils some desirable properties for a market including individual rationality (i.e., each  
44 participant has a non-negative payoff from entering the market) and budget balance (i.e., the overall  
45 amount of prices paid and received by participants sums up to zero), and it can be implemented through  
46 two alternative distributed approaches that do not require airlines to disclose confidential information.  
47 Later, Granberg and Polishchuk (2012) show how to design mechanisms that can be used for the allocation  
48 of many different types of ATM resources, including ATFM slots. Even though these mechanisms are  
49 socially optimal (i.e., resources are distributed in the way that best serves the users community as a  
50 whole), truthful (i.e., each individual user has incentive to play fairly), and, under certain assumptions,  
51 individually rational, they are not budget balanced because the resource owner gains profit from the users’  
52 payments. Other truthful market mechanisms for ATFM slot allocation are proposed by Rosenthal and  
53 Eisenstein (2016) and by Mehta and Vazirani (2020). However, these mechanisms are centralised and  
54 therefore - even if no airline has an incentive to misreport the delay costs of its flights - airlines are  
55 forced to reveal information that they prefer to keep to themselves. To simultaneously respect this  
56 request for confidentiality and still involve airlines in the ATFM slot allocation process, for some years  
57 now EUROCONTROL<sup>1</sup> has been developing UDPP, the User Driven Prioritisation Process (Pilon et al.,  
58 2016, 2019; Ruiz et al., 2019a). This mechanism requires that each AU associates a priority value to  
59 each of its flights, on the basis of which the FPFS allocation can then be modified (intra-airline). No  
60 inter-airline exchanges are allowed, but in certain circumstances an AU can also get a slot that did not  
61 previously belong to it and thus obtain a substantial reduction in the cost of the associated delay. ~~Each~~  
62 ~~AU is also free not to participate in the UDPP; in this case its FPFS allocation is not changed. UDPP has~~  
63 ~~received a wide consensus among airlines and has reached a high level of maturity after several human~~  
64 ~~in the loop validation exercises. Besides a study addressing an outdated version of UDPP, the current~~  
65 ~~version is purely empirical since it is not supported, as far as we know, by any methodological framework~~  
66 ~~that can quantify or at least estimate a priori the benefits that this mechanism could bring in terms of~~  
67 ~~cost reduction with respect to FPFS. Each AU can choose not to participate in the UDPP, and if they do,~~  
68 ~~their FPFS allocation remains unchanged. UDPP has gained widespread acceptance among airlines and~~  
69 ~~has become highly refined after numerous validation exercises involving human in the loop simulations~~

---

<sup>1</sup>EUROCONTROL, the European Organisation for the Safety of Air Navigation, is the international organisation that develops and maintains an efficient air traffic management across Europe.

(SESAR, 2019). However, it is important to note that the assessment of the performance of the current version of UDPP is based solely on empirical data. Indeed, we have not found any established framework that can quantitatively or predictively assess the cost reduction benefits of this mechanism compared to FPPS. The only study we found regarding this mechanism was related to an outdated version (Zhang et al., 2021).

All the models that have been presented in this short review foresee the allocation of slots to a single capacitated resource. In the not infrequent case, however, that one or more flights are subject to several regulations (our analysis of traffic data shows that in the week 1-7 July 2019 47% of regulated flights are subject to more than one regulation, see Section 5.2), Barnhart et al. (2012) demonstrate with a simple example that performing FPPS for each resource independently can produce inconsistencies, i.e., a regulation may impose on a flight an ATFM slot that is not compatible with the slot imposed on the same flight by another regulation. It is therefore necessary to propose alternative algorithms. In Europe, for instance, when a flight is subject to multiple regulations, the delay of the Most Penalising Regulation (MPR), meaning the one causing the highest delay, takes precedence and is forced into all other regulations. In the U.S. other heuristics (named *precedence RBS* and *exemption RBS*) are applied (Barnhart et al., 2012).

Our contribution fits into this context as it outlines a market-based approach to minimise the cost of ATFM delays in the presence of multiple regulations, guaranteeing to airlines the confidentiality of their costs. We introduce a time interval, which we refer to as *time window*, associated to each regulation a flight is subject to. A flight is expected to enter every regulated resource it has to traverse within its corresponding time window. A set (or bundle) of time windows is initially allocated to each flight, and the time windows of this bundle are possibly traded to form another bundle that decreases the flight delay cost. This exchange can be guided by a central authority, **assuming it has access to the cost information of the flights**, or carried out in a distributed manner without the need for each flight to communicate the costs of the delay. Our numerical computations based on real data instances of a test day of the European airspace show that the market-based allocation may reduce the delay costs from 47% up to 89% with respect to the initial allocation, while preserving cost confidentiality.

The idea of characterising the trajectory of a flight by a set of time windows is not entirely new in the ATM context, either at the execution (while en-route) (Berechet et al., 2009; Han et al., 2010; Margellos and Lygeros, 2013; Rodríguez-Sanz et al., 2019, 2020) or tactical planning (on the day of operations) phases of a flight (Castelli et al., 2011a). More recently, the definition of a flight trajectory as a sequence of time windows allowed Bolić et al. (2021a,b) to quantify the flexibility that can be granted to flights at the strategic level (up to 6 months ahead) taking into account changing airspace configurations and capacity. Flights complying with time windows guarantee that they will not impact negatively any other flight.

None of these studies considers the time windows that characterise the flight trajectory as objects that can be traded in order to improve a system objective, such as the overall cost of the ATFM delay of flights subject to multiple regulations. A first hint of how to solve this latter problem was provided by Castelli et al. (2011c), which is now significantly refined and extended in this paper in several aspects, including the formulation of the distributed market mechanism, and its detailed implementation and resolution. Furthermore, we provide a realistic characterisation of the European airspace in terms of traffic, airspace configuration and cost data, as described in Section 5. Finally, all computational experiments are run on real data.

The remainder of this paper unfolds as follows. Section 2 introduces the main features of Air Traffic Management, and describes the algorithm currently in place to allocate ATFM slots. The approach followed when airlines make available to an authority the costs incurred when their flights are delayed is presented in Section 3, which mathematically defines (a) the centralised allocation of time window

117 bundles that minimises the overall cost of delay and (b) the market mechanism that allows to trade  
118 the bundles of an initial allocation and reach the minimum ATFM delay cost allocation. The model  
119 relies on an integer linear programming formulation. If, on the other hand, the costs of the delay cannot  
120 be revealed, the allocation and trading of the time window bundles can be carried out in a distributed  
121 manner. Section 4 develops the distributed model by applying the Lagrangian relaxation technique and  
122 the subgradient method. Section 5 describes how the dataset for the numerical experimentation was  
123 prepared, and Section 6 reports computational results on some subsets of the dataset. Section 7 contains  
124 the conclusions and some ideas for further development of this work.

## 125 2. Some key concepts of Air Traffic Management

126 ATM is an extremely complex system, which has to cope with very different situations in daily  
127 operations (Niarchakou and Sfyroeras, 2021; Cook, 2016). The evaluation of the proposed market mech-  
128 anism can therefore only be based on a simplified representation of ATM, especially with regard to slot  
129 allocation procedures (Section 2.1).

130 The whole airspace is divided in *ATC sectors* (or simply, *sectors*), which define the area of responsi-  
131 bility of air traffic controllers. Adjacent sectors can be merged into *collapsed* sectors from time to time,  
132 in order to enable more effective use of resources. Sectors which are not collapsed are called *elementary*  
133 sectors.

134 ~~The capacity of airspace resources is the ability of the ATM system to provide air navigation services~~  
135 ~~to a certain volume of air traffic by meeting safety standards. In particular,~~ In Europe the capacity of  
136 an ATC sector is defined as the maximum number of aircraft that can enter the given sector during a  
137 specified period of time (usually one hour), while permitting an acceptable level of air traffic controller  
138 workload.

139 If traffic demand in an airspace or airport is forecast to exceed capacity, the NM decides whether to  
140 apply flow restrictions. Flow restrictions, called ATFM regulations, ~~impose delays to aircraft~~ **restrict the**  
141 **departure times of flights, assigning them controlled take-off times (CTOTs) -which may cause delays on**  
142 **some flights-**, so that traffic is smoothed and avoid overload of the regulated sector or airport.

143 ATFM regulations are based on the principle that delays are both safer and less costly to be absorbed  
144 on the ground rather than in the air. Therefore, any delay forecast in a capacity-constrained resource  
145 along a flight's route is anticipated at the departure airport before take-off, a practice known as *ground-*  
146 *holding* (Odoni, 1987). The flight receives an *ATFM slot* (also called *departure slot*), a 15-minute time  
147 range during which the aircraft must take off.

### 148 2.1. The allocation of ATFM slots

149 In this section, we present the main principles of the slot allocation procedures. ATFM slots are man-  
150 aged by the Computer Assisted Slot Allocation (CASA) system, which is a largely automatic and cen-  
151 tralised tool run by EUROCONTROL. CASA initially calculates an Estimated Take-Off Time (ETOT)  
152 for each flight. This enables each flight to be given an Estimated Time Over (ETO), **which is** the point  
153 of entry at each sector through which the route is planned.

154 A regulation is characterised by a period of activation (start and end time), the **allowed** entering  
155 flow rate (in flights per hour), and some other specifications. The regulation is divided by CASA into  
156 a number of slots of equal width depending on the rate. Each regulation is thus associated to a Slot  
157 Allocation List which is initially empty. Normally the capacity of each slot is equal to one flight, although  
158 in special circumstances it may be higher (Ruiz et al., 2019b).

159 The policy under which flights are assigned slots is First Planned First Served (FPFS). CASA sorts  
160 the flights entering the regulation according to their ETO over the restricted location, and assigns a slot  
161 to each flight in this sequential order, as close as possible to the ETO.

162 This order is also maintained when a flight is subject to multiple regulations by giving precedence to  
163 the regulation causing the highest delay, i.e., the Most Penalising Regulation (MPR). The flight receives  
164 an ATFM slot according to the FPFS order applied to the MPR. ~~The delay thus obtained is then forced~~  
165 ~~into all other regulations.~~ **The delay resulting from the MPR is used to find a slot in the other regulations**  
166 **crossed by the flight such that it is the closest to the new ETO of the flight in those regulated sectors.**  
167 **The flight is then “forced” into the slots predetermined by the MPR without following the FPFS logic**  
168 **in those regulations.**

169 The FPFS policy on which the CASA system is based is considered fair and equitable by all parties  
170 involved (Lulli and Odoni, 2007). However, from an efficiency point of view, it is not optimal as it  
171 does not consider the impact of ATFM delays to airlines in terms of delay costs. If one considers the  
172 economical impact of ATFM delays on the flight profitability, there is typically a trade-off between  
173 fairness and efficiency (Barnhart et al., 2012).

174 ~~Moreover, CASA works in a passive mode from the point of view of airspace users, since ATFM~~  
175 ~~slots are imposed by a central authority.~~ **Moreover, in the current CASA logic (MPR-FPFS), the airspace**  
176 **users remain as passive actors, since they receive ATFM slots that are calculated and assigned to them**  
177 **based on pre-existing flight plan information and with limited options to influence the slot sequences**  
178 **based on the impact of the resulting delays to their operations and daily schedules.** ~~In contrast, an~~  
179 ~~important tool to implement~~ **To fix that, an important concept that could be implemented to optimise**  
180 **the cost of the** ATFM measures is Collaborative Decision Making (CDM), a process in which decisions  
181 are agreed by all stakeholders who actively take part in the decision-making (Niarchakou and Sfyroeras,  
182 2021). In particular, since the cost of delay for a flight is possibly known only by the airline operating it,  
183 the allocation of ATFM slots would benefit from an enhanced application of CDM. In this context, our  
184 proposal is to introduce a mechanism for exchanging slots. Since it would be impossible to replicate the  
185 operational reality with absolute precision, we have adopted certain simplifications. For example, the  
186 capacity of each TW is always equal to 1 and never higher as is sometimes the case, or the procedure for  
187 FPFS allocation of bundles can be called a CASA-like algorithm as it certainly follows the MPR rationale,  
188 but is not identical to the CASA algorithm (see Appendix C and also section 3). Thus, the objects that  
189 are exchanged, although very similar, do not inherit exactly all the dynamics and characteristics of the  
190 actual slots. In order not to misuse the term ‘slots’, we refer to these objects as *time windows* (TWs) in  
191 the rest of the paper.

## 192 2.2. The cost of delays in ATM

193 On the day of operations, various factors cause flight delay, for example weather, ATFM measures,  
194 and issues attributable to aircraft operators. There are two main types of costs that airlines experience  
195 due to delays: strategic delay costs and tactical delay costs. Strategic costs are mainly due to schedule  
196 buffers, while tactical costs are those incurred on the day of operations due to actual delays.

197 A major component in the tactical cost of delay that impacts on airlines are the costs associated with  
198 delayed passengers, which fall into two categories: *hard* costs and *soft* costs. Hard costs are determined  
199 by passenger re-booking, compensation and care. Soft costs are due to the loss of market share that  
200 comes from passenger dissatisfaction.

201 Tactical costs also include maintenance and crew costs. Tactical maintenance costs are due for  
202 example to the mechanical attrition of aircraft waiting at gates, whereas tactical crew costs are based  
203 on the cost of crewing for additional minutes above those planned at the strategic phase.

204 For maintenance and crew costs, one minute of delay does not depend on the extent of the delay. In  
205 contrast, longer passenger delays have higher associated costs per minute than shorter ones, thus making  
206 tactical costs a super-linear function of delay length.

207 A comprehensive study on the costs of delays in the air traffic management system was carried out  
208 for EUROCONTROL by Cook et al. (2004), and then updated and extended in subsequent years (Cook



209 and Tanner, 2015; Cook et al., 2021). It estimates cost delay figures for different phases of flight (e.g.  
210 en-route and at-gate), for a range of specific aircraft types and three cost scenarios (low, base and high),  
211 separately for strategic and tactical delays. **These estimations will be used as inputs in this research (see**  
212 **Section 5).**

### 213 3. The central resource allocation problem

214 This section formalises the market mechanism for the TW allocation by a central authority when  
215 flights are subject to multiple regulations. We first describe in mathematical terms the time window  
216 bundle allocation that minimises the cost of the delay as faced by the central authority (Sections 3.1  
217 and 3.2). This minimum cost allocation is then confronted with the initial allocation that is currently  
218 granted. With a slight abuse of terminology, we refer to it as *FPFS allocation* (see Section 5.2 and  
219 Appendix C for details on its implementation that mimics the Most Penalising Regulation principle).  
220 In particular, Section 3.3 introduces a mechanism for the allocation of time window bundles to flights,  
221 alternative to FPFS, which is cost-efficient. The mechanism is market-based since airlines can be seen as  
222 competitors contending for a limited resource, which is the capacity of regulated sectors or airports. In  
223 addition, it satisfies some of the following properties commonly used in mechanism design (see Krishna,  
224 2009, for a formal treatment):

- 225 1. Individual rationality: each individual receives a non-negative utility from participating in the  
226 mechanism, so that it is preferable to participate than not participate.
- 227 2. Budget balance: the mechanism requires no financing from outside. In particular, a mechanism  
228 is strongly budget balanced if the total payment of the participants is equal to zero. The mech-  
229 anism neither receives subsidisation from outside, nor generates a surplus; it just redistributes  
230 money among participants. A mechanism is weakly budget balanced if the total payment of the  
231 participants is larger or equal than zero: the mechanism can potentially generate a surplus.
- 232 3. Allocative efficiency: the mechanism maximises the sum of individual utilities.
- 233 4. Incentive compatibility: the best strategy for participants is to report their valuations truthfully.  
234 No agent can increase their utility by misreporting their true preferences.

235 ~~However, due to the impossibility theorem by Myerson and Satterthwaite (1983) the four properties~~  
236 ~~cannot be satisfied at the same time. Myerson and Satterthwaite (1983) showed that in the presence of~~  
237 ~~asymmetric information (i.e. the value of a given good for a given agent is only known by such agent),~~  
238 ~~it is not always possible that the above four properties are guaranteed. Indeed, under some specific~~  
239 ~~conditions and assumptions, Myerson and Satterthwaite proved that it is impossible to find a market~~  
240 ~~mechanism that can satisfy all four properties simultaneously.~~ The mechanism proposed in Section (3.3)  
241 relaxes the fourth property, and thus assumes that participants report their preferences honestly to the  
242 central authority. Section 4 will describe a distributed implementation of such mechanism in which  
243 participants are assumed to act honestly introducing their preferences in a privacy-preserving manner.  
244 The validity of this assumption is addressed in Appendix A.

#### 245 3.1. Mathematical formulation

246 The proposed mathematical formulation requires the notation introduced in Table 1.



---

$\mathcal{F}$	set of flights
$\mathcal{R}$	set of regulations
$K_r$	capacity of regulation $r \in \mathcal{R}$ (in flights per hour)
$start_r$	start time of regulation $r \in \mathcal{R}$
$end_r$	end time of regulation $r \in \mathcal{R}$
$L_r$	TW allocation list of regulation $r \in \mathcal{R}$
$\Delta_r$	TW width (in minutes) of regulation $r \in \mathcal{R}$
$N_r$	number of TWs of regulation $r \in \mathcal{R}$
$I_j$	lower bound of the $j$ -th TW in $L_r$
$U_j$	upper bound of the $j$ -th TW in $L_r$
$\epsilon$	time discretisation interval
$\hat{L}_r$	augmented TW allocation list of regulation $r \in \mathcal{R}$
$n_f$	number of regulations crossed by flight $f \in \mathcal{F}$
$R_f$	list of the regulations crossed by flight $f \in \mathcal{F}$
$r_i$	$i$ -th regulation crossed by flight $f \in \mathcal{F}$
$E_f$	list of the expected times of entry of flight $f \in \mathcal{F}$
$e_i$	expected entry time into $r_i$
$Q_f$	set of feasible bundles of flight $f \in \mathcal{F}$
$q_f$	an element of $Q_f$ , i.e., $q_f \in Q_f$ is a feasible bundle for flight $f$
$d_{q_f}$	delay of bundle $q_f$
$C(f, q_f)$	cost of bundle $q_f$ for flight $f$

---

Table 1: Model's notation

247 We consider a set of flights  $\mathcal{F}$  that are scheduled within a period of time  $\mathcal{T}$ , and a set of regulations  
248  $\mathcal{R}$  active during  $\mathcal{T}$  that limit the rate of flights entering a capacity constrained resource, either an airport  
249 or an airspace sector.

250 Each regulation  $r \in \mathcal{R}$  has a capacity of  $K_r$  flights per hour and is active for a time period  
251  $[start_r, end_r]$ . Each regulation  $r$  is associated to a *TW allocation list*  $L_r$ , a list of time windows of  
252 equal width that depends on the capacity. The TW width, expressed in minutes, is

$$\Delta_r = \frac{60}{K_r}$$

253 and given that the duration  $end_r - start_r$  is expressed also in minutes, the number of time windows is

$$N_r = \left\lfloor \frac{(end_r - start_r)}{\Delta_r} \right\rfloor$$

254 where  $\lfloor \cdot \rfloor$  denotes rounding to the nearest integer.

255 For  $j = 1, \dots, N_r$  the time interval associated to the  $j$ -th TW of the list  $[I_j, U_j] \in L_r$  is given by

$$I_j = start_r + \lfloor (j-1) \cdot \Delta_r \rfloor$$

$$U_j = \begin{cases} I_{j+1} - \epsilon & \text{for } j = 1, \dots, N_r - 1. \\ end_r & \text{for } j = N_r. \end{cases}$$

256  
257 where  $\epsilon = 1$  second and the rounding is applied to an argument expressed in seconds (for example, an  
258 argument of 1 hour, 10 minutes, 3 seconds and 15 hundredths of a second is rounded to 1 hour, 10  
259 minutes and 3 seconds).

260 The interval  $[start_r, end_r]$  is thus partitioned into a set of disjoint segments, with a time discretization  
261 of 1 second. Since  $\lfloor x \rfloor < x + 1$  for any positive real number  $x$ , we have that

$$\left\lfloor \frac{(end_r - start_r)}{\Delta_r} \right\rfloor - 1 < \frac{(end_r - start_r)}{\Delta_r}$$

262 and thus

$$(N_r - 1) \cdot \Delta_r < (end_r - start_r).$$

263 Since  $\lfloor x \rfloor < \lfloor y \rfloor$  for any  $0 < x < y$  and since  $start_r$  and  $end_r$  are reported with a precision of one minute  
264 in our data, i.e.  $(end_r - start_r) = \lfloor end_r - start_r \rfloor$ , it follows

$$\lfloor (N_r - 1) \cdot \Delta_r \rfloor < (end_r - start_r)$$

265 so we conclude that  $I_{N_r} < end_r$ .

266 The time discretization is actually not necessary for the optimisation model, but it simplifies the  
267 bundle construction algorithm (appendix B).

268 Hereinafter, a TW will be denoted interchangeably by an integer  $j$  representing its position in the  
269 list  $L_r$ , or an interval  $[I_j, U_j]$ .

270 Each TW has capacity of 1 flight and represents the time interval in which a flight is allowed to enter  
271 the regulated resource during its regulated period. However, a flight is also allowed to enter a regulated  
272 resource before or after its regulated period. To deal with the two situations uniformly, we augment the  
273 TW allocation list of each regulation  $r$  with two “dummy” time windows  $j = 0$  and  $j = N_r + 1$  defined  
274 by

$$I_0 = -\infty, \quad U_0 = start_r - \epsilon$$

275

$$I_{N_r+1} = end_r + \epsilon, \quad U_{N_r+1} = +\infty.$$

276 To simplify the model formulation, we assume these two additional time windows, placed at the beginning  
277 and at the end of  $L_r$ , have infinite capacity, so that the number of flights that they can accommodate is  
278 not limited. Let us call  $\hat{L}_r$  the TW allocation list augmented in this way,  $\hat{L}_r = [0, 1, 2, \dots, N_r + 1]$ .

279 The flight plan of each flight  $f \in \mathcal{F}$  individuates a list  $R_f = [r_1, \dots, r_{n_f}]$  of the regulations crossed  
280 along the route of  $f$  from its departure to its destination, and a list  $E_f = [e_1, \dots, e_{n_f}]$  of the expected  
281 times of entry into each regulated resource. The list  $E_f$  is defined with respect to the original (pre-  
282 regulated) flight plan and its  $i$ -th element  $e_i$  is the expected time of entry into the  $i$ -th element  $r_i$  of  $R_f$ .  
283 The length of the two lists  $n_f = |R_f|$  is the number of regulations affecting flight  $f$ .

284 One time window must be assigned to each flight  $f \in \mathcal{F}$  for each regulated resource it crosses. A  
285 dummy time window is also a feasible assignment. We denote this *bundle* of time windows by  $q_f =$   
286  $[TW_1, \dots, TW_{n_f}]$  where  $TW_i \in \hat{L}_{r_i}$  for  $i = 1, \dots, n_f$ .

287 Since we assume that flights cannot be anticipated, every time window in  $q_f$  must end after the  
288 corresponding entry time of  $f$ , i.e.  $e_i \leq U_{TW_i}$  for all  $i = 1, \dots, n_f$ .

289 If  $n_f > 1$ , we assume that the flying time  $e_{i+1} - e_i$  between consecutive resources  $r_i$  and  $r_{i+1}$ , for  
290  $i = 1, \dots, n_f - 1$ , is fixed. A bundle  $q_f$  is compatible with the fixed flying times if there exists a sequence  
291 of time instants  $[t_1, \dots, t_{n_f}]$  such that  $I_{TW_i} \leq t_i \leq U_{TW_i}$  for all  $i = 1, \dots, n_f$  and  $t_{i+1} - t_i = e_{i+1} - e_i$   
292 for all  $i = 1, \dots, n_f - 1$ . The sequence  $[t_1, \dots, t_{n_f}]$  represents the re-planned times of entry in each  
293 regulated resources and is a temporal shift of the trajectory  $[e_1, \dots, e_{n_f}]$ . Among the possible sequences  
294  $[t_1, \dots, t_{n_f}]$ , for each  $TW_i$  the smallest shift occurs when  $t_i = I_{TW_i}$ . Therefore, the *delay*  $d_{q_f}$  experienced  
295 by flight  $f$  due to bundle  $q_f$  is due to the time window that leads to the largest among these smallest  
296 shifts. Specifically,

$$d_{q_f} = \max_{i=1, \dots, n_f} \min_{t_i} \{(t_i - e_i)^+ : I_{TW_i} \leq t_i \leq U_{TW_i}\} = \max_{i=1, \dots, n_f} \{(I_{TW_i} - e_i)^+\} \quad (1)$$

297 being  $(\cdot)^+ = \max\{\cdot, 0\}$ . The delay is strictly positive if  $e_i < I_{TW_i}$  for at least one  $TW_i \in q_f$ .

298 A delay  $d_{q_f}$  causes to flight  $f$  a cost  $C(f, q_f)$ , which is a non-linear non-decreasing function of the  
 299 delay, and depends on the flight  $f$  through factors such as type of aircraft and number of passengers.

300 We say that a bundle  $q_f$  is feasible for  $f$  if either  $q_f$  is empty, and in this case  $f$  is cancelled, or it  
 301 satisfies the following requirements:

- 302 (i) it contains a time window  $TW_i$  for each regulation in  $R_f$  and  $E_i \leq U_{TW_i}$  component-wise;
- 303 (ii) it is compatible with the fixed flying times;
- 304 (iii) the delay is acceptable, i.e. it satisfies the bound  $d_{q_f} \leq MaxDel_f$  where  $MaxDel_f$  is the delay  
 305 beyond which it is more convenient to cancel  $f$ .

306 We denote by  $Q_f$  the set of all feasible bundles for flight  $f$ . Appendix B describes a simple algorithm  
 307 for constructing the set  $Q_f$ .

### 308 3.2. The optimal allocation

309 The allocation of time windows to flights that minimises the total cost of delay is given by the optimal  
 310 solution of the following binary optimisation problem (TW allocation problem):

$$\min \sum_{f \in \mathcal{F}} \sum_{q \in Q_f} C(f, q)x(f, q) \quad (2a)$$

$$\sum_{f \in \mathcal{F}} \sum_{q \in Q_f: q \ni k} x(f, q) \leq 1 \quad \forall r \in \mathcal{R}, k \in L_r \quad (2b)$$

$$\sum_{q \in Q_f} x(f, q) = 1 \quad \forall f \in \mathcal{F} \quad (2c)$$

$$x(f, q) \in \{0, 1\} \quad \forall f \in \mathcal{F}, q \in Q_f \quad (2d)$$

311 The objective function (2a) minimises the sum of all delay costs. Constraint (2b) is the capacity  
 312 constraint, which guarantees that no more than one flight is assigned to any time window. Constraint  
 313 (2c) is the allocation constraint, which guarantees that every flight receives one and only one bundle  
 314 from its set of requests. Constraint (2d) is the integrality constraint. The variable  $x(f, q)$  is equal to one  
 315 when flight  $f$  is assigned to bundle  $q$ , and zero otherwise. Problem (2) is *NP*-hard as we can reduce to  
 316 it the *NP*-complete Maximal Independent Set (MIS) problem (Lawler et al., 1980).

317 A feasible solution of problem (2) always exists, because for all  $f \in \mathcal{F}$ ,  $Q_f$  always contains either the  
 318 empty bundle corresponding to flight cancellation, or the bundle composed of all “dummy” time windows  
 319 that consumes no capacity.

320 The allocation given by the application of the optimal solution of problem (2) will be denoted by  
 321  $\mathcal{X}^* = \{q_f^*\}_{f \in \mathcal{F}}$ . The allocation  $\mathcal{A} = \{a_f\}_{f \in \mathcal{F}}$  given by the FPFS rule constitutes a feasible solution of  
 322 problem (2).

323 In the particular case when  $|\mathcal{R}| = 1$  and flights compete for time windows in a single capacity  
 324 constrained resource  $r$ , problem (2) simplifies into the following:

$$\min \sum_{f \in \mathcal{F}} \sum_{k \in Q_f} C(f, k)x(f, k) \quad (3a)$$

$$\sum_{f \in \mathcal{F}} \sum_{k \in Q_f} x(f, k) \leq 1 \quad \forall k \in L_r \quad (3b)$$

$$\sum_{k \in Q_f} x(f, k) = 1 \quad \forall f \in \mathcal{F} \quad (3c)$$

$$x(f, k) \geq 0 \quad \forall f \in \mathcal{F}, k \in Q_f \quad (3d)$$

325 The integrality constraint was dropped since, in this case, the solutions of the linear relaxation are  
 326 automatically integral. The reason is that problem (3) has the form of an assignment problem, and so  
 327 the constraint matrix is totally unimodular.

328 In presence of a single regulation, the FPFS allocation  $\mathcal{A}$  minimises the total delay, or in other words  
 329  $\mathcal{A}$  is an optimal solution of problem (3) when  $C(f, k) = d_k$  (Castelli et al., 2011b). This fact is no longer  
 330 true in presence of many interacting regulations (Ruiz et al., 2019c).

331 For what will follow in the next section, it is convenient to reformulate problem (2) in terms of  
 332 maximisation of a total value, instead of minimisation of a total cost. Let us define the *value* of a bundle  
 333  $q$  to flight  $f$  as the difference between the cost of the bundle  $a_f$  assigned to  $f$  under the FPFS, and the  
 334 cost of  $q$ :

$$V(f, q) = C(f, a_f) - C(f, q). \quad (4)$$

335 The value is positive if  $q$  causes a delay smaller than the delay of  $a_f$ , and negative otherwise. Then, we  
 336 consider the following problem:

$$Z_{IP} = \max \sum_{f \in \mathcal{F}} \sum_{q \in Q_f} V(f, q)x(f, q) \quad (5a)$$

$$\sum_{f \in \mathcal{F}} \sum_{q \in Q_f: q \ni k} x(f, q) \leq 1 \quad \forall r \in \mathcal{R}, k \in L_r \quad (5b)$$

$$\sum_{q \in Q_f} x(f, q) = 1 \quad \forall f \in \mathcal{F} \quad (5c)$$

$$x(f, q) \in \{0, 1\} \quad \forall f \in \mathcal{F}, q \in Q_f \quad (5d)$$

337 Trivially, problem (5) is equivalent to problem (2) in the sense that their optimal solution is the same,  
 338 because the objective function only differs by a constant term. In fact,

$$\begin{aligned} \sum_{f \in \mathcal{F}} \sum_{q \in Q_f} (C(f, a_f) - C(f, q))x(f, q) &= \sum_{f \in \mathcal{F}} C(f, a_f) \sum_{q \in Q_f} x(f, q) - \sum_{f \in \mathcal{F}} \sum_{q \in Q_f} C(f, q)x(f, q) \\ &= \sum_{f \in \mathcal{F}} C(f, a_f) - \sum_{f \in \mathcal{F}} \sum_{q \in Q_f} C(f, q)x(f, q) \end{aligned}$$

339 where the last equality follows from constraint (5c).

### 340 3.3. Pricing the exchange

341 The allocation  $\mathcal{X}^*$  given by the optimal solution of problem (5) could be perceived as unfair by  
 342 airlines, because it is not always true that  $C(f, q_f^*) \leq C(f, a_f)$ , or in other terms the utility  $V(f, q_f^*)$  can  
 343 be negative. Some flights reduce their delay with respect to the FPFS while some other increase their  
 344 delay. In order to design a mechanism which is both allocative efficient and individual rational, as well  
 345 as weakly budget balanced, we introduce the possibility of payments between airlines that accompany  
 346 the optimal allocation and attach a price  $p(q_f^*)$  to each bundle  $q_f^* \in \mathcal{X}^*$ . In this way, airlines who are  
 347 penalised by the optimal allocation with respect to the FPFS receive a monetary compensation, whereas  
 348 airlines who are better off after the implementation of the optimal allocation can possibly be charged for  
 349 the delay reduction.

350 In order to find a set of prices  $\mathcal{P}^* = \{p(q_f^*)\}_{f \in \mathcal{F}}$  that support the optimal exchange, if we consider  
 351 the optimal solution found for the linear relaxation of problem (5), the values of the associated dual  
 352 variables are optimal for the following problem:

$$Z_{LP} = \min \sum_{f \in \mathcal{F}} u(f) + \sum_{r \in \mathcal{R}} \sum_{k \in L_r} \pi(k) \quad (6a)$$

$$u(f) + \sum_{r \in \mathcal{R}} \sum_{k \in L_r: k \in q} \pi(k) \geq V(f, q) \quad \forall f \in \mathcal{F}, q \in Q_f \quad (6b)$$

$$\pi(k) \geq 0 \quad \forall r \in \mathcal{R}, k \in L_r \quad (6c)$$

Variables  $\pi(k)$  are the dual variables associated to the capacity constraint (5b) and  $u(f)$  are the dual variables associated to the assignment constraint (5c). Variables  $\pi(k)$  can be interpreted as prices of time windows, and  $u(f)$  can be interpreted as utilities of users. It is then natural to assume a linear pricing of bundles, so that  $p(q) = \sum_{k \in q} \pi^*(k)$  where  $\pi^*(k)$  are the optimal dual variables. If we also assume that the utility of a flight when assigned a bundle  $q_f$  is  $-C(f, q_f) - p(q_f)$ , a market mechanism that charges  $p(q_f^*)$  to each flight  $f$  for the assigned bundle  $q_f^*$  would not satisfy individual rationality, because some flights would incur a greater cost with  $q_f^*$  than with  $a_f$  and additionally be forced to make a payment.

In order to fulfil individual rationality, we consider the allocation  $a_f$  as an endowment guaranteed to all flights. Then the market mechanism, mediated by the central authority, takes place in two steps:

1. First, the FDFS bundles  $\mathcal{A}$  are allocated for free, as in the current system.
2. Next, the optimal allocation  $\mathcal{X}^*$  is implemented and the dual prices are charged for the bundle exchange: each flight pays  $p(q_f^*)$  for the assigned bundle  $q_f^*$  and receives the price  $p(a_f)$  for the released time windows in  $a_f$ .

For flight  $f$  the cost after step 1 is  $C(f, a_f)$ , and the cost after step 2 is  $C(f, q_f^*) + p(q_f^*) - p(a_f)$ . Therefore the utility variation of  $f$  when taking part in the mechanism is  $\Delta u(f) = C(f, a_f) - C(f, q_f^*) + p(a_f) - p(q_f^*)$ . Now we show the condition under which the individual rationality condition  $\Delta u(f) \geq 0$  holds.

The complementary slackness conditions between the linear relaxation of problem (5) and its dual (6) are

$$x^*(f, q) > 0 \implies u^*(f) + \sum_{r \in \mathcal{R}} \sum_{k \in L_r: k \in q} \pi^*(k) = V(f, q) \quad \forall f \in \mathcal{F}, q \in Q_f \quad (7a)$$

$$\sum_{f \in \mathcal{F}} \sum_{q \in Q_f: q \ni k} x^*(f, q) < 1 \implies \pi^*(k) = 0 \quad \forall r \in \mathcal{R}, k \in L_r \quad (7b)$$

If the optimal solution of the linear relaxation of (5) is integer, then the optimal allocation  $\{q_f^*\}_{f \in \mathcal{F}}$  satisfies

$$u^*(f) = V(f, q_f^*) - p(q_f^*) \quad (8a)$$

$$u^*(f) \geq V(f, q) - p(q) \quad \forall q \in Q_f \quad (8b)$$

Equation (8a) follows from complementary slackness (7a) and equation (8b) follows from the feasibility (6b) of the optimal solution. Putting them together yields

$$V(f, q_f^*) - p(q_f^*) \geq V(f, q) - p(q) \quad \forall q \in Q_f \quad (9)$$

In particular, since  $\mathcal{A}$  is a feasible solution, taking  $q = a_f$  gives

$$\Delta u(f) = C(f, a_f) - C(f, q_f^*) + p(a_f) - p(q_f^*) \geq 0 \quad (10)$$

378 which is the property of individual rationality: every agent has a non-negative profit when selling its  
 379 FPFS bundle  $a_f$  and buying  $q_f^*$ . Equation (9) says that not only flight  $f$  prefers bundle  $q_f^*$  over  $a_f$ , but  
 380 also over every other bundle  $q \in Q_f$ .

381 Now we show that the complementary slackness conditions are sufficient to impose that the weak  
 382 budget balance property holds, i.e.,

$$\sum_{f \in \mathcal{F}} (p(q_f^*) - p(a_f)) \geq 0. \quad (11)$$

383 Let us define  $\mathcal{L} = \bigcup_{r \in \mathcal{R}} L_r$  the set of all time windows. Equation (7b) says that every time window  
 384 which is unassigned under the optimal solution  $\mathcal{X}^*$  has a price zero. It follows that

$$\sum_{f \in \mathcal{F}} p(q_f^*) = \sum_{k \in \mathcal{L}} \pi^*(k) \quad (12)$$

385 where (5b) has also been used. So the net turnout resulting from the market mechanism is

$$\sum_{f \in \mathcal{F}} (p(q_f^*) - p(a_f)) = \sum_{k \in \mathcal{L}} \pi^*(k) - \sum_{f \in \mathcal{F}} \sum_{k \in a_f} \pi^*(k) = \sum_{k \in \mathcal{L} \setminus \bigcup_{f \in \mathcal{F}} a_f} \pi^*(k) \geq 0. \quad (13)$$

386 Taking a closer look at how the mechanism works, consider the monetary flow associated to each  
 387 time window  $k \in \mathcal{L}$ . There are four cases:

- 388 (i) If  $k$  is assigned both under the FPFS allocation  $\mathcal{A}$  and under the optimal allocation  $\mathcal{X}^*$ , respectively  
 389 to flight  $f$  and to flight  $g$ , then  $f$  sells time window  $k$  to  $g$  at the price  $\pi^*(k)$  and the central authority  
 390 is not involved in the exchange.
- 391 (ii) If  $k$  is assigned under  $\mathcal{A}$  to a flight  $f$  and it is unassigned under  $\mathcal{X}^*$ , then  $f$  receives  $\pi^*(k)$  from  
 392 the central authority, but  $\pi^*(k) = 0$  due to complementary slackness (7b).
- 393 (iii) If  $k$  is not assigned under  $\mathcal{A}$  but it is assigned to a flight  $g$  under  $\mathcal{X}^*$ , then  $g$  pays  $\pi^*(k) \geq 0$  to the  
 394 central authority.
- 395 (iv) If  $k$  is not assigned in  $\mathcal{A}$  nor in  $\mathcal{X}^*$ , then there is no monetary flow associated to it.

396 Again, from this reasoning it follows that the total revenue for the central authority is larger or equal to  
 397 zero. The mechanism can produce a surplus, but not incur a deficit. In presence of a single regulation  
 398  $|\mathcal{R}| = 1$ , Castelli et al. (2011b) proved that  $\sum_{f \in \mathcal{F}} (p(q_f^*) - p(a_f)) = 0$  and the mechanism is strongly  
 399 budget balanced. They also showed that case (iii) cannot happen for  $|\mathcal{R}| = 1$ , because all time windows  
 400 that are unassigned under  $\mathcal{A}$  are also unassigned under  $\mathcal{X}^*$ .

401 Equations (9) and (12) together show that the allocation  $\mathcal{X}^* = \{q_f^*\}_{f \in \mathcal{F}}$  and the prices  $\mathcal{P}^* =$   
 402  $\{p(q_f^*)\}_{f \in \mathcal{F}}$  form a Walrasian equilibrium and  $\mathcal{P}^*$  is the set of market-clearing prices (Bikhchandani  
 403 and Mamer, 1997). However, the complementary slackness conditions (7a) and (7b) can guarantee that  
 404 the individual rationality and weak budget balance properties hold only in the case that the duality gap  
 405 between problem (5) and its linear relaxation is zero. Otherwise, the integer optimal solution of problem  
 406 (5) is not guaranteed to form a Walrasian equilibrium with the prices given by the optimal solution of  
 407 (6). In particular, problem (6) may estimate utility values that are greater than the actual ones. Under  
 408 these circumstances, it can be decided that initially only a subset of flights are allowed to exchange time  
 409 windows so that a smaller problem for which the zero duality gap holds is considered, see Section 6.5. All  
 410 flights belonging to this subset are allowed to exchange time windows and prices are negotiated between  
 411 airlines. We remark that in the case of a unique regulation, the individual rationality and strong budget  
 412 balance properties always hold, because problem (3) always gives integer optimal solutions, as mentioned  
 413 in Section 3.2.

414 **4. A distributed market mechanism**

415 The market mechanism described in Section 3.3 is a centralised model for the allocation of time  
 416 windows to flights and the calculation of supporting prices. It requires that the central authority, who is  
 417 in charge of solving problem (5), has complete knowledge of the delay cost data  $C(f, q) \forall f \in \mathcal{F} \forall q \in Q_f$ ,  
 418 which can be possibly evaluated for each flight only by its aircraft operator. However, the cost of delay  
 419 for flights represent confidential information in the commercially competitive air transport industry, and  
 420 airlines could be reluctant to communicate their delay costs to the central authority.

421 This section develops a decentralised version of the market mechanism, which does not require the  
 422 explicit disclosure of private information by airlines, and instead allows to elicit their preferences in an  
 423 indirect way. This mechanism also relieves the central authority of the burden of solving the NP-hard  
 424 problem (5) by relaxing it into a set of trivial problems, one for each flight  $f \in \mathcal{F}$  (see problem (17)  
 425 below). The solution to these latter problems is then attributed to the airlines operating the flights to  
 426 prevent the explicit disclosure of private information.

427 Throughout the section we make use of well-known Lagrangian relaxation theory results and we refer  
 428 the reader unfamiliar with them to, e.g., Fisher (2004).

429 *4.1. The Lagrangian dual of the allocation problem*

430 The Lagrangian relaxation of problem (5) with respect to the capacity constraint (5b) is

$$Z_{LR}(\lambda) = \max \sum_{f \in \mathcal{F}} \sum_{q \in Q_f} V(f, q)x(f, q) + \sum_{k \in \mathcal{L}} \lambda_k \left( 1 - \sum_{f \in \mathcal{F}} \sum_{q \in Q_f: q \ni k} x(f, q) \right) \quad (14a)$$

$$\sum_{q \in Q_f} x(f, q) = 1, \quad \forall f \in \mathcal{F} \quad (14b)$$

$$x(f, k) \geq 0, \quad \forall f \in \mathcal{F}, k \in Q_f \quad (14c)$$

$$\lambda_k \geq 0, \quad \forall k \in \mathcal{L} \quad (14d)$$

431 where  $\lambda_k$  are the Lagrangian multipliers. The second term in the objective function (14a) has the role of  
 432 penalising capacity violations. The integrality constraint (5d) has been dropped because the constraint  
 433 matrix of problem (14) is totally unimodular.

434 It is convenient to rewrite objective function (14a) in an alternative form:

$$\begin{aligned} & \sum_{f \in \mathcal{F}} \sum_{q \in Q_f} V(f, q)x(f, q) + \sum_{k \in \mathcal{L}} \lambda_k \left( 1 - \sum_{f \in \mathcal{F}} \sum_{q \in Q_f: q \ni k} x(f, q) \right) = \\ & = \sum_{f \in \mathcal{F}} \sum_{q \in Q_f} V(f, q)x(f, q) - \sum_{f \in \mathcal{F}} \sum_{q \in Q_f} \sum_{k \in q} \lambda_k x(f, q) + \sum_{k \in \mathcal{L}} \lambda_k = \\ & = \sum_{f \in \mathcal{F}} \sum_{q \in Q_f} \left[ V(f, q) - \sum_{k \in q} \lambda_k \right] x(f, q) + \sum_{k \in \mathcal{L}} \lambda_k \end{aligned} \quad (15)$$

435 Equation (15) shows that problem (14) is separable into  $|\mathcal{F}|$  problems, one for each  $f \in \mathcal{F}$ . The  
 436 Lagrangian subproblem for flight  $f$  is

$$Z_{LR}(f, \lambda) = \max \sum_{q \in Q_f} \left[ V(f, q) - \sum_{k \in q} \lambda_k \right] x(f, q) \quad (16a)$$

$$\sum_{q \in Q_f} x(f, q) = 1 \quad (16b)$$

$$x(f, k) \geq 0 \quad \forall k \in Q_f \quad (16c)$$



437 and  $Z_{LR}(\lambda) = \sum_{f \in \mathcal{F}} Z_{LR}(f, \lambda) + \sum_{k \in \mathcal{L}} \lambda_k$ . Each subproblem for  $f \in \mathcal{F}$  can be locally solved by the  
 438 airline operating  $f$ .

439 Problem (16) can be solved in linear time by inspection as

$$Z_{LR}(f, \lambda) = \max_{q \in Q_f} \left\{ V(f, q) - \sum_{k \in q} \lambda_k \right\}, \quad (17)$$

440 always corresponding to optimal integer values for the variables  $x(f, k)$  in (16).

441 We can interpret  $\sum_{k \in q} \lambda_k$  as the cost of a bundle  $q$  according to the prices  $\lambda$ . The optimal solution of  
 442 problem (17) is the bundle  $q \in Q_f$  that maximises the utility of  $f$  if we interpret Lagrangian multipliers  
 443 as prices of time windows.

444 The Lagrangian dual of problem (5) is

$$Z_{LD} = \min_{\lambda \geq 0} Z_{LR}(\lambda) \quad (18)$$

445 Since the formulation (14) is totally unimodular,  $Z_{LD} = Z_{LP}$  and the optimal Lagrange multipliers that  
 446 solve problem (18) are optimal dual variables for the linear relaxation of problem (5). Hence, if the  
 447 duality gap between problem (5) and its linear relaxation is null,  $Z_{LD} = Z_{LP} = Z_{IP}$  and the optimal  
 448 Lagrange multipliers are equilibrium prices that support the optimal exchange.

449 We solve problem (18) via the subgradient method (Fisher, 2004, Section 6). First of all, the central  
 450 authority fixes the initial prices  $\lambda^0$ , for example  $\lambda^0 = 0$ . Then the subgradient method proceeds in an  
 451 iterative way. At iteration  $t$ , each flight  $f$  determines the bundle  $q_f^{*t}$  that maximises its utility variation  
 452 when exchanging the FPFS endowment  $a_f$  with another bundle  $q \in Q_f$ , at the current prices  $\lambda^t$ :

$$q_f^{*t} = \operatorname{argmax}_{q \in Q_f} \left\{ V(f, q) - p^t(q) \right\} = \operatorname{argmax}_{q \in Q_f} \left\{ V(f, q) - p^t(q) + p^t(a_f) \right\} \quad (19)$$

453 where  $p^t(q) = \sum_{k \in q} \lambda_k^t$ . Notice that  $f$  only needs to communicate the optimal solution  $x^t$  of (14)  
 454 according to prices  $\lambda^t$ , i.e. its most preferred bundle  $q_f^{*t}$ , and not the optimal value  $Z_{LR}(f, \lambda)$  to the  
 455 central authority.

456 Then the central authority computes the following quantity

$$SG_k^t = 1 - \sum_{f \in \mathcal{F}} \sum_{q \in Q_f: q \ni k} x^t(f, q) \quad \forall k \in \mathcal{L}. \quad (20)$$

457 The vector  $SG^t$  is a subgradient of  $Z_{LR}(\lambda)$  at the point  $\lambda^t$ . The sum in (20) represents the number  
 458 of flights whose demanded bundle  $q_f^{*t}$  contains time window  $k$ . Then the prices are centrally updated  
 459 according to

$$\lambda_k^{t+1} = \max(0, \lambda_k^t - \mu_t SG_k^t) \quad \forall k \in \mathcal{L} \quad (21)$$

460 where  $\mu_t$  is the step length and will be discussed in Section 4.2.

461 Equation (21) has the following interpretation: for each  $k \in \mathcal{L}$

462 (i) if  $SG_k^t < 0$ , the demand for time window  $k$  exceeds the capacity, so the price of  $k$  is raised;

463 (ii) if  $SG_k^t > 0$ , less capacity is used than available, so the price of  $k$  is lowered;

464 (iii) if  $SG_k^t = 0$ , there is already a balance between demand and capacity, so the price is unchanged.

465 The market mechanism is configured in a series of exchanges of information between the central  
 466 authority and the aircraft operators. Each iteration proceeds as follows:

- 467 1. The central authority communicates prices  $\lambda^t$  to all aircraft operators.
- 468 2. Each aircraft operator solves problem (16) according to prices  $\lambda^t$  and communicates the demanded  
469 bundle  $q_f^{*t}$  to the central authority.
- 470 3. The central authority computes the imbalance between the demand  $q_f^{*t}$  and the capacity of time  
471 windows according to equation (20) and updates the prices of time windows  $\lambda^t$  according to (21).

472 In the rest of this Section, we discuss the details of the iterative market mechanism, i.e., of the  
473 subgradient method applied to problem (18). Hereinafter, we call *(IP)* the problem (5), *(LP)* its linear  
474 relaxation, *(LR( $\lambda$ ))* the problem (14) and *(LD)* the problem (18).

#### 475 4.1.1. Termination of the iterative market mechanism

476 Under appropriate choice of the stepsize the subgradient algorithm converges to the optimal solution  
477 of *(LD)*.

478 If at iteration  $t$  the bundles demanded by flights happen to form an allocation  $x^t$  that respects the  
479 capacity, i.e.  $SG_k^t \geq 0 \forall k \in \mathcal{L}$ , or in other words  $q_f^{*t}$  share no time windows, then the allocation will  
480 constitute a feasible solution for *(IP)*. Indeed, thanks to property (19), the prices  $\lambda^t$  are such that  
481 the exchange is individual rational, and each user also maximises the individual utility. However, we  
482 remark that there is no guarantee that the prices satisfy the weak budget balance property (11). It can  
483 occur that the solution  $x^t$  of problem *(LR( $\lambda^t$ ))* is feasible but not optimal for *(IP)*. In this case, the  
484 complementary slackness conditions do not hold.

485 If the solution is not only capacity-compliant but also satisfies complementary slackness  $SG^t \cdot \lambda^t = 0$ ,  
486 i.e. all unassigned time windows have zero price, then  $Z_{LR}(\lambda^t) = Z_{IP}$ , so  $x^t$  is an optimal solution of *(IP)*  
487 and  $\lambda^t$  is an optimal solution of problem (6), they form a Walrasian equilibrium, and the subgradient  
488 algorithm stops.

489 When the duality gap  $Z_{LD} - Z_{IP}$  is zero, an optimal solution  $(\lambda^*, x^*)$  always exists, i.e.,  $(\lambda^*, x^*)$   
490 feasible for *(LD)* and *(IP)* and such that the complementary slackness conditions hold. Unfortunately,  
491 determining the value of  $x^*$  may be not easy even when the subgradient algorithm makes the sequence  
492  $\lambda^t$  converge to  $\lambda^*$ . In presence of multiple optimal solutions for *(LR( $\lambda^*$ ))*, each optimal solution of *(IP)*  
493 is among the optimal solutions of *(LR( $\lambda^*$ ))*, but the opposite is not necessarily true. Hence, the solution  
494 of *(LR( $\lambda^*$ ))* may provide an assignment  $x$  which is not optimal for *(IP)*.

495 Generally speaking, there is no way of proving that the subgradient algorithm has converged to the  
496 optimal values  $\lambda^*$ . To resolve this difficulty, the method is usually terminated upon reaching an arbitrary  
497 iteration limit (Fisher, 2004).

#### 498 4.2. Choice of stepsize

499 A choice of a stepsize for the subgradient method that guarantees convergence to the minimum of  
500 the Lagrangian function is

$$\mu_t = \frac{\epsilon_t (Z_{LR}(\lambda^t) - Z_{LP})}{\|SG^t\|^2} \quad (22)$$

501 where  $0 < \epsilon < \epsilon_t \leq 2$ . In (22) the numerator depends on the difference between the current Lagrangian  
502 objective function value and the minimum of the Lagrangian function, and the denominator is the square  
503 norm of the subgradient vector. Unfortunately, in general, the minimum of the Lagrangian function is  
504 unknown and one uses a lower bound on this minimum. In our case, both  $Z_{LP}$  and  $Z_{LR}(\lambda^t)$  are unknown  
505 because the objective function coefficients of the Lagrangian function  $V(f, q)$  (the costs of delay) are  
506 unknown to the central authority. The rest of this Section proposes a way to compute an estimate for  
507 the difference  $Z_{LR}(\lambda^t) - Z_{LP}$  to be used in the stepsize formula.

508 4.2.1. Cost elicitation

509 First of all, we discuss how the preferences communicated by airlines through (19) during the course of  
 510 the distributed market mechanism actually provide information on costs  $C(f, q)$  to the central authority.

511 Recall that  $p^t(q) = \sum_{k \in Q} \lambda_k^t$  is the price of a bundle  $q$  at iteration  $t$ . Equation (19) says that for all  
 512  $f \in \mathcal{F}$

$$V(f, q_f^{*t}) - V(f, q) \geq p^t(q_f^{*t}) - p^t(q) \quad \forall q \in Q_f \quad (23)$$

513 The right-hand side of equation (23) is a known quantity, whereas the left-hand side is unknown. Equa-  
 514 tion (23) represents a set of  $|Q_f|$  inequalities each involving the values of a pair of bundles. At every  
 515 iteration, we can add a new set of  $|Q_f|$  inequalities for each  $f \in \mathcal{F}$  and build up a system of inequalities  
 516 incrementally. Notice that, however, the total number of inequalities collected by the end of the iterative  
 517 market mechanism is limited, because if at some iteration  $t$  the bundle demanded by  $f$  happens to be  
 518 the same bundle demanded at an earlier iteration  $t' < t$ , i.e.  $q_f^{*t} = q_f^{*t'}$ , then we can simply update the  
 519 right-hand side of the old inequalities instead of adding a new set of inequalities, if the new right-hand  
 520 side is larger than the old one.

521 We can also take advantage of the fact that the cost is a non-decreasing function of the delay to write  
 522 an additional relation between values:

$$V(f, q) \geq V(f, \bar{q}) \quad \forall q \in Q_f, \bar{q} \in Q_f : d_q < d_{\bar{q}} \quad (24)$$

523 In addition, from Equation (4) it follows that  $V(f, a_f) = C(f, a_f) - C(f, a_f)$  so

$$V(f, a_f) = 0. \quad (25)$$

524 The system of inequalities (23) together with (24) and (25) defines  $\forall f \in \mathcal{F}$  a convex polyhedron in  
 525 a  $|Q_f|$ -dimensional space which gets smaller during the course of iterations, and which contains a point  
 526 corresponding to the real combination of values  $V(f, q) \forall q \in Q_f$ . This polyhedron represents all the  
 527 information that has been elicited about the cost of delay for flight  $f$ . Now let  $q_1, q_2, \dots, q_{|Q_f|}$  be the  
 528 bundles in  $Q_f$  ordered by increasing delay. One can obtain a lower bound  $LB(f, q) \leq V(f, q)$  on the  
 529 value of each bundle  $q \in Q_f$  by exploiting this elicited information. The tightest possible lower bound is  
 530 the solution of the following linear program, whose constraints define the polyhedron described before

$$LB^t(f, q_k) = \min v(q_k) \quad (26a)$$

$$v(q_i) - v(q_j) \geq c_{ij}^t \quad \forall q_i \in Q_f, q_j \in Q_f \quad (26b)$$

$$v(q_{i-1}) \geq v(q_i) \quad \forall q_i \in Q_f \setminus \{q_1\} \quad (26c)$$

$$v(a_f) = 0 \quad (26d)$$

531 Constraints (26b) correspond to equations (23), constraints (26c) correspond to equations (24) and (26d)  
 532 to (25). The coefficients of constraints (26b) are updated at each iteration as follows: for all  $q_j \in Q_f$

$$c_{ij}^t = \begin{cases} c_{ij}^{t-1} & \text{if } q_i \neq q_f^{*t} \\ \max(p^t(q_i) - p^t(q_j), c_{ij}^{t-1}) & \text{if } q_i = q_f^{*t} \end{cases} \quad (27)$$

533 initialised at  $t = 0$  with

$$c_{ij}^0 = -\infty \quad \forall q_i \in Q_f, q_j \in Q_f \quad (28)$$

534 Similarly, changing the objective function (26a), one obtains an upper bound  $UB(f, q) \geq V(f, q)$  for  
 535 all  $q \in Q_f$

$$UB^t(f, q_k) = \max v(q_k) \quad (29a)$$

$$v(q_i) - v(q_j) \geq c_{ij}^t \quad \forall q_i \in Q_f, q_j \in Q_f \quad (29b)$$

$$v(q_{i-1}) \geq v(q_i) \quad \forall q_i \in Q_f \setminus \{q_1\} \quad (29c)$$

$$v(a_f) = 0 \quad (29d)$$

536 Notice that in doing this, we are effectively eliciting information on costs, but only the information  
537 which is necessary for the subgradient procedure to converge, and the bounds are not strict generally.

538 If we reformulate the cost elicitation problem in terms of costs instead of values, we can write an  
539 additional relation between them: not only we know that the cost function is non-decreasing, but also  
540 that it is superlinear. This means that the *unit* cost of delay is a non-decreasing function of the delay:

$$\frac{C(f, q)}{d_q} \leq \frac{C(f, \bar{q})}{d_{\bar{q}}} \quad \forall q \in Q_f, \bar{q} \in Q_f : d_q < d_{\bar{q}}, d_q \neq 0 \quad (30)$$

541 This is a linear constraint, thus it can be included in our linear problem, and it makes constraint (24)  
542 redundant, since it is stricter. Relation (25) is substituted by

$$C(q) = 0 \quad \text{if } d_q = 0 \quad (31)$$

543 Then problem (26) becomes

$$\widetilde{LB}^t(f, q_k) = \min c(q_k) \quad (32a)$$

$$c(q_j) - c(q_i) \geq c_{ij}^t \quad \forall q_i \in Q_f, q_j \in Q_f \quad (32b)$$

$$d_{q_i} \cdot c(q_{i-1}) \leq d_{q_{i-1}} \cdot c(q_i) \quad \forall q_i \in Q_f \setminus \{q_1\} \quad (32c)$$

$$c(q_2) \geq 0 \quad (32d)$$

$$c(q_1) = 0 \quad (32e)$$

544 We conclude this subsection with a word of caution. Even though the distributed mechanism does  
545 not require “explicit” disclosure of delay costs, the arguments presented in this subsection show how  
546 a central authority could estimate these values based on the bundles communicated by the airlines  
547 during the algorithm iterations. The quality of the estimate depends on the number of different bundles  
548 observed: the fewer the number of bundles, the worse the estimates. In Section 6.4 we shows on an  
549 example data instance that the estimates obtained are rough in almost all cases, therefore there is no  
550 risk of cost information disclosure in practice.

#### 551 4.2.2. Computation of the stepsize

552 Returning to the problem of choosing an appropriate stepsize for the subgradient method, a possible  
553 approach would be to compute an upper bound on  $Z_{LR}(\lambda^t)$  and a lower bound on  $Z_{LP}$  based on the  
554 upper and lower bounds on values obtained in Section 4.2.1, and plug these bounds in equation (22). In  
555 particular, at each iteration  $t$  a lower bound  $ZLB^t \leq Z_{LP}$  can be computed as

$$ZLB^t = \max \sum_{f \in \mathcal{F}} \sum_{q \in Q_f} LB^t(f, q) x(f, q) \quad (33a)$$

$$\sum_{f \in \mathcal{F}} \sum_{q \in Q_f : q \ni k} x(f, q) \leq 1 \quad \forall r \in \mathcal{R}, k \in L_r \quad (33b)$$

$$\sum_{q \in Q_f} x(f, q) = 1 \quad \forall f \in \mathcal{F} \quad (33c)$$

$$x(f, q) \geq 0 \quad \forall f \in \mathcal{F}, q \in Q_f \quad (33d)$$

556 See Appendix D.1 for a proof that problem (33) indeed provides a lower bound on  $Z_{LP}$ . An upper bound  
 557  $ZUB^t(\lambda^t) \geq Z_{LR}(\lambda^t)$  can be computed as

$$ZUB^t(\lambda^t) = \sum_{f \in \mathcal{F}} UB^t(f, q_f^{*t}) + SG^t \cdot \lambda^t \quad (34)$$

558 since  $Z_{LR}(\lambda^t) = \sum_{f \in \mathcal{F}} V(f, q_f^{*t}) + SG^t \cdot \lambda^t$ . It follows that  $ZUB^t(\lambda^t) - ZLB^t \geq Z_{LR}(\lambda^t) - Z_{LP}$ . Then  
 559 the stepsize is computed as

$$\mu_t = \frac{\epsilon_t (ZUB^t(\lambda^t) - ZLB^t)}{\|SG^t\|^2} \quad (35)$$

560 Problem (33) has always a finite optimal value since  $a_f$  is a feasible solution and  $LB^t(f, a_f) = 0$ , so  
 561  $ZLB^t \geq 0$ . However, problem (29) can be unbounded and so it can happen that  $ZUB^t(\lambda^t) = +\infty$ , thus  
 562 this method is not viable. In Ranieri (2010) a method is proposed to compute a looser lower bound on  
 563  $V(f, q)$  without solving the linear problem (26), but he does not provide a way to compute an upper  
 564 bound on  $Z_{LR}(\lambda^t)$ .

565 Now we propose another method to compute the stepsize, which instead is always viable. The idea  
 566 is to estimate the difference  $Z_{LR}(\lambda^t) - Z_{LP}$  directly, instead of estimating bounds on  $Z_{LR}(\lambda^t)$  and  $Z_{LP}$   
 567 separately and then taking the difference. First of all, we can write

$$Z_{LR}(\lambda^t) - Z_{LP} = \sum_{f \in \mathcal{F}} V(f, q_f^{*t}) + SG^t \cdot \lambda^t - \max_{x \in S} \sum_{f \in \mathcal{F}} \sum_{q \in Q_f} V(f, q) x(f, q) \quad (36)$$

568 where  $S$  is the set of solutions  $x$  satisfying constraints (5b) and (5c). Thanks to (5c) we can write

$$Z_{LR}(\lambda^t) - Z_{LP} = SG^t \cdot \lambda^t - \max_{x \in S} \sum_{f \in \mathcal{F}} \sum_{q \in Q_f} (V(f, q) - V(f, q_f^{*t})) x(f, q) \quad (37)$$

569 The maximisation problem appearing in (37) involves differences between values  $V(f, q) - V(f, q_f^{*t})$ . A  
 570 finite upper bound on these quantities is readily available thanks to equation (23). This gives a finite  
 571 lower bound on  $Z_{LR}(\lambda^t) - Z_{LP}$  (due to the minus sign in front of the maximum) that can be plugged in  
 572 the stepsize formula.

573 More precisely, once we have  $UB_{diff}^t(f, q) \geq V(f, q) - V(f, q_f^{*t})$  obtained as

$$UB_{diff}^t(f, q) = p^t(q) - p^t(q_f^{*t}) \quad (38)$$

574 we can solve the following linear problem

$$ZUB_{diff}^t = \max \sum_{f \in \mathcal{F}} \sum_{q \in Q_f} UB_{diff}^t(f, q) x(f, q) \quad (39a)$$

$$\sum_{f \in \mathcal{F}} \sum_{q \in Q_f: q \ni k} x(f, q) \leq 1 \quad \forall r \in \mathcal{R}, k \in L_r \quad (39b)$$

$$\sum_{q \in Q_f} x(f, q) = 1 \quad \forall f \in \mathcal{F} \quad (39c)$$

$$x(f, q) \geq 0 \quad \forall f \in \mathcal{F}, q \in Q_f. \quad (39d)$$

575 To simplify the notation, let us define the *residual*

$$RES^t = SG^t \cdot \lambda^t - ZUB_{diff}^t \quad (40)$$

576 which will satisfy  $RES^t \leq Z_{LR}(\lambda^t) - Z_{LP}$  (see again Appendix D.1). Finally we set

$$\mu_t = \epsilon_t \frac{RES^t}{\|SG^t\|^2}. \quad (41)$$

577 It can be proved (see Appendix D.2) that  $RES^t \geq 0$  and so the stepsize is non-negative, whenever the  
578 duality gap  $Z_{IP} - Z_{LD}$  is zero. Therefore, in that case, there is no risk that a step of subgradient iteration  
579 moves in the opposite direction of  $-SG^t$ .

580 The bounds  $UB_{diff}^t(f, q)$  obtained with (23) can be improved by exploiting the ordered structure of  
581  $Q_f$  (the monotonicity of cost functions). They are updated recursively with

$$\widehat{UB}_{diff}^t(f, q_i) = \begin{cases} p^t(q_i) - p^t(q_f^{*t}) & \text{for } i = 1 \\ \min(p^t(q_i) - p^t(q_f^{*t}), \widehat{UB}_{diff}^t(f, q_{i-1})) & \text{for } i = 2, \dots, |Q_f| \end{cases} \quad (42)$$

582 Then we can leverage the information obtained at previous iterations to write

$$UB_{diff}^t(f, q_i) = \min(\widehat{UB}_{diff}^t(f, q_i), UB_{diff}^{t'}(f, q_i)) \quad \forall q_i \in Q_f \text{ for } t' < t \text{ if } q_f^{*t'} \geq q_f^{*t} \quad (43)$$

583 Of course, the tightest possible upper bound on  $V(f, q) - V(f, q_f^{*t})$  can be found by solving a linear  
584 problem analogous to (29)

$$UB_{diff}^t(f, q_k) = \max v(q_k) - v(q_f^{*t}) \quad (44a)$$

$$v(q_i) - v(q_j) \geq c_{ij}^t \quad \forall q_i \in Q_f, q_j \in Q_f \quad (44b)$$

$$v(q_{i-1}) \geq v(q_i) \quad \forall q_i \in Q_f \setminus \{q_1\} \quad (44c)$$

$$v(a_f) = 0 \quad (44d)$$

585 but the combination of (42) and (43) allows to drastically reduce the computational cost, and will be  
586 used to present the results in Section 6.

587 Similarly one could find a lower bound  $LB_{diff}^t(f, q) \leq V(f, q) - V(f, q_f^{*t})$  and use it to compute an  
588 upper bound on  $Z_{LR}(\lambda^t) - Z_{LP}$  to be used in the stepsize formula. However this does not always work  
589 because there could not exist a feasible solution  $x \in S$  for which  $\sum_{f \in \mathcal{F}} \sum_{q \in Q_f} LB_{diff}^t(f, q)x(f, q) > -\infty$ .

590 The downside of this method is the computational cost of solving a linear problem (39) at every  
591 iteration of the subgradient method.

## 592 5. Data collection

### 593 5.1. Traffic data

594 We tested the model on real traffic data collected from the Demand Data Repository (DDR2) of  
595 EUROCONTROL. In particular (Niarchakou and Sfyroeras, 2021),

- 596 • Each regulation is characterised by its associated traffic volume<sup>2</sup>, the sub-periods in which it is  
597 divided and the capacities of each sub-period.
- 598 • Each flight is characterised by: aircraft type, airline, ATFM delay, most penalising regulation,  
599 departure airport and destination airport, Estimated Take-Off Time (ETOT) and Estimated Time  
600 of Arrival (ETA), and the list of *intersections*, i.e., the estimated times of entry into each sector  
601 crossed along the flight route according to the *Initial Trajectory*, also called M1 trajectory, which  
602 is based on the Last Filed Flight Plan from the aircraft operator.

---

<sup>2</sup>A *traffic volume* is a tool used in ATFM to select a specific volume of air traffic. It is related to an aerodrome or an airspace sector, and to one or more traffic flows that can be either included or excluded from the regulation.

603 5.2. Data extraction

604 We processed the data about all flights and regulations on the 4th of July 2019 in all Europe. There  
605 were a total of 39080 flights and 203 regulations during that day. We selected data relative to one day  
606 because there are typically few regulations at night, so it is unlikely to have a regulation straddling the  
607 midnight.

608 As a preprocessing stage, we excluded flights having the same origin and destination airport, flights  
609 with unknown origin or destination airport, and regulations with zero capacity. The resources used  
610 to execute each flight  $f$  are the intersected airspace sectors, the departure airport and the destination  
611 airport; we are interested only in the regulated resources. In order to form the set  $R_f$  (see Section 3.1),  
612 we selected the resources for which the following three conditions hold:

- 613 (i) the resource is regulated;
- 614 (ii) the time of entry into the resource falls within the regulation period;
- 615 (iii) the flight is not excluded from the regulation by the corresponding traffic volume definition.

616 In the case the resource is an airspace sector, the time of entry in point (ii) is the ETO over the sector  
617 taken from the intersections; in the case the resource is the departure airport, the time of entry is the  
618 ETOT, and in the case the resource is the arrival airport, the time of entry is the ETA. The times of  
619 entry in each resource will constitute the inputs  $E_f$  of the model together with  $R_f$ . Point (ii) requires  
620 another specification: if the flight is subject to more than one regulation, we actually require that the  
621 interval  $[e_i, e_i + MaxDel_f]$  (where  $e_i$  is the time of entry) intersects with the regulation period, because  
622 due to the delay in the Most Penalizing Regulation the flight may be pushed inside the regulation period  
623 even if the time of entry was before the start of the regulation. That is why in Section 3.1 we included  
624 a “dummy” time window at the beginning of a regulation, and not only at the end.

625 Point (iii) means that we check whether the flight is captured by the flows associated to the traffic  
626 volume. In addition, if the resource is the departure airport, we check that the traffic volume does not  
627 capture only inbound flights, and vice versa for the destination airport.

628 Since airspace sectors are sometimes non-convex, it can happen that a flights enters into a sector  
629 more than once. In these cases, we kept only the first intersection with the sector.

630 Regulations can be applied to collapsed sectors, but intersections of flights are always with elementary  
631 sectors. We verified that for our test day (4 July 2019), for each regulation associated with a collapsed  
632 sector, the opening schemes indicate that all elementary sectors of that collapsed sector were active during  
633 the time interval in which that regulation was in force. Since an elementary sector can be included in  
634 more than one collapsed sector, but only one of them can be active at a given time, we could associate  
635 each collapsed sector with the elementary sectors composing it (the configuration, i.e. the structure of  
636 collapsed sectors, was available from the data) and we considered a flight subject to a regulation on a  
637 collapsed sector if the flight crosses an elementary sector inside it.

638 Let  $F$  be the subset of flights which are found to be associated to at least one regulation according  
639 to our analysis, i.e. the flights for which  $R_f \neq \emptyset$ . We obtained  $|F| = 11354$ . Finally, let  $F' \subset F$  be  
640 the subset of flights departing from outside the ATFM Area (which includes States receiving the full  
641 ATFM service from EUROCONTROL) and the ATFM Adjacent Area (which includes FIRs adjacent  
642 to the ATFM Area) and exempted flights (e.g. official, humanitarian and emergency flights). These  
643 categories of flights are not subject to ATFM measures. We did not include airborne flights (which are  
644 also not subject to the ATFM slot allocation) in  $F'$  because the data did not specify the time of creation  
645 of regulations. We obtained  $|F'| = 1016$ . For each flight  $f \in F'$ , for each  $r_i \in R_f$ , we blocked the TW of  
646  $r_i$  containing  $e_i$ , meaning that no other flight can be assigned this TW in the optimal allocation. Flights  
647 in  $F'$  will not participate in the market mechanism. If a flight *does not wish* to join, but prefers to keep



648 its FPFS time window, it can be excluded from the market by placing it in the set  $F'$  (see also Appendix  
 649 A). For each  $f \in F \setminus F'$ , a bundle containing any blocked time window is considered not feasible.

650 On our test day, on average, a flight in  $F \setminus F'$  crosses 1.6 regulations and 39% of flights are subject  
 651 to more than one regulation (see Figure 1, which shows the number of regulations crossed by a flight).  
 652 Figure 2 shows a cumulative histogram of the number of flights subject to a regulation. The average is  
 653 85, and only 16% of cases comprise more than 150 flights. Based on these histograms, to test the market  
 654 mechanism on meaningful real instances, in Section 6 we used the examples of two regulations with a  
 655 number of flights each not too small but also not too large as the latter cases are rare (see also Table 3).  
 656 Applications on larger instances can be found in Appendix E. We extended the analysis of traffic data  
 657 for seven days (from the 1st to the 7th of July 2019) and found that a regulated flight crosses on average  
 658 1.9 regulations and 47% of regulated flights are subject to more than one regulation, thus motivating the  
 659 need for a multiple regulation allocation system such as the one proposed in this work.

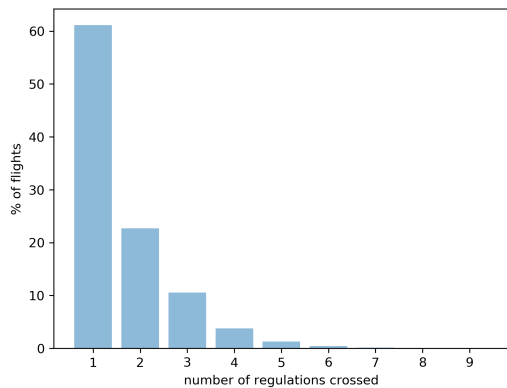


Figure 1: Normalised histogram of the number of regulations crossed by flights in  $F \setminus F'$ , 4 July 2019

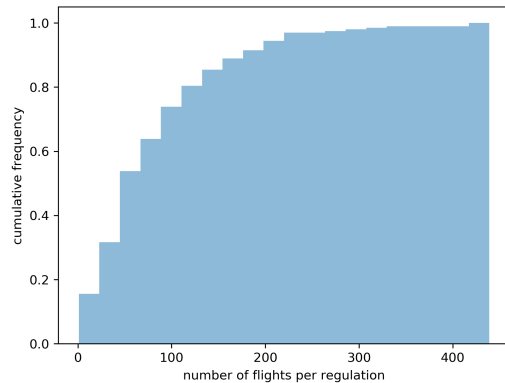


Figure 2: Normalised cumulative histogram of the number of flights in  $F \setminus F'$  subject to a regulation, 4 July 2019

660 In principle, it would have been possible to use the ATFM delay from the data to obtain the FPFS  
 661 TW allocation. However, the resulting allocation would not respect the capacities of time windows,  
 662 because it was impossible to reproduce exactly the real environment due to the intricacies of the ATM  
 663 system rules, which we tried nevertheless to take into account to the best of our possibilities. Thus we  
 664 applied the algorithm in Appendix C instead.

665 As a check, we compared the set  $R_f$  obtained for each flight with the Most Penalising Regulation  
 666 indicated in the data. For 98% of the flights the MPR was included in  $R_f$ . In addition, there was a  
 667 small number of flights for which we found  $R_f \neq \emptyset$  but the MPR was not present in the data, meaning  
 668 that the flight was not subject to any regulation in reality; we decided to ignore these flights.

669 For reasons of computational efficiency, the size of  $Q_f$  was limited by setting  $MaxDel_f = 60 \text{ min } \forall f \in$   
 670  $\mathcal{F}$ . This is reasonable since the typical ATFM delays are below 60 minutes.

671 As a last note, it is straightforward to adapt the construction of TW allocation lists for regulations  
 672 having more than one sub-period. We build a TW list as described in Section 3.1 for each sub-period,  
 673 and then the allocation list  $L_r$  is the union of all these TW lists.

### 674 5.3. Cost data

675 As anticipated in Section 2.2, delay costs can be estimated relying on the values reported in Cook  
 676 et al. (2021). To reflect the likely range of costs, they are assigned under three scenarios (“low”, “base”  
 677 and “high”) for four flight phases (at-gate, taxi, en-route and arrival management), and are calculated  
 678 for 18 common types of aircraft. In this work, we only consider the at-gate tactical delays.

679 To assign delay costs to flights whose aircraft is not among the 18 reference types, aircraft in the  
680 data were clustered in 18 groups whose centroid is the reference type, based on the square root of the  
681 Maximum Take-Off Weight (MTOW), as in Bolić et al. (2017).

682 Flights of low cost airlines were assigned to the low cost profile, flights into a hub airport were assigned  
683 to the high profile, and all other flights to the base profile, as in Bolić et al. (2017).

684 We attached the cost of delay specifically to each regulated flight, based on the aircraft type, company,  
685 destination, and flight length, which are available from the data. We also attached the cost of cancellation  
686 which was estimated in Cook et al. (2021) as well. Due to the clustering, many flights have the same  
687 cost of delay, which is unrealistic, thus we added a small Gaussian zero-mean noise to each cost  $C(f, q)$ .

## 688 6. Computational results

689 All algorithms were coded in Python and making use of NumPy, a package for scientific computing.  
690 All experiments were performed using the FICO XPRESS optimisation software, version 8.12.3. It is a  
691 software specifically devoted to solving mixed-integer linear programming problems. We ran it on a 64  
692 bit Intel(R) Xeon(R) W-2145 @3.70GHz 16 core CPU computer, having 31 GB of RAM memory and  
693 Ubuntu 20.04 operating system. On this architecture, the most computationally demanding example  
694 instance presented here (Section 6.5) took 105 seconds to execute.

695 First of all, we recall the formula (41) for the stepsize in the subgradient method elaborated in Section  
696 4.2.2:

$$\mu_t = \epsilon_t \frac{RES^t}{\|SG^t\|^2}. \quad (45)$$

697 In addition to formula (45), we experimented with a heuristic method to adapt the stepsize, which we  
698 now describe. The idea is not to use  $RES^t$  directly in the stepsize formula, but just to monitor the trend  
699 of the Lagrangian function during iterations. We initialise  $\mu_0$  as in (45). Then, we half  $\mu_t$  every time the  
700 objective function fails to improve after a given number of iterations  $n$  according to the estimate given  
701 by  $RES^t$ , and at least  $n$  iterations have passed since the last time we halved  $\mu_t$ . That is:

$$\mu_{t+1} = \begin{cases} \frac{\mu_t}{\gamma} & \text{if } RES^{t-i} \geq RES^{t-n} \text{ and } \mu_t = \mu_{t-i} \quad \forall i = 0, \dots, n-1 \\ \mu_t & \text{otherwise} \end{cases} \quad (46)$$

702 with  $\gamma = 2$ , and  $\mu_0 = \epsilon_0 \frac{RES^0}{\|SG^0\|^2}$ . This piece-wise constant stepsize can be seen as a modification of a  
703 common rule used in the subgradient method, which halves the stepsize every  $\nu$  iterations for some fixed  
704  $\nu$ . In this case,  $\nu$  is dynamically adapted based on the behaviour of the function. The parameters  $n$  and  
705  $\epsilon_0$  need to be tuned, and we found that  $n = 4$  and  $\epsilon_0 = 3$  work well in general. We will use these values  
706 in the rest of this Section if not otherwise stated.

707 A rule of thumb to initialise  $\lambda^t$  is to set  $\lambda^0$  at random uniformly in an interval corresponding roughly  
708 to the range of equilibrium prices, which can be determined after a number of trials on similar-sized  
709 instances. We observed that generally setting  $\lambda^0$  at random works better than setting  $\lambda^0 = 0$ . We  
710 believe that this is because in this way initial prices are on average closer to their final equilibrium value,  
711 which makes convergence faster.

712 To illustrate the computational experience gained, we describe the results obtained on some instances  
713 involving two regulations and extracted from the real data (Section 5), which are representative of the  
714 average case (see Figures 1 and 2). We first discuss the convergence of the subgradient depending on  
715 the different stepsizes (45) - (46) and conclude that the best choice is to rely on the heuristic approach  
716 (section 6.1). This is the stepsize used in the subsequent examples. In the first case, we present an  
717 instance producing a weakly budget balanced solution (section 6.2), then a case where the subgradient  
718 does not converge and therefore TW capacity is not respected (section 6.3). Since we observe a decreasing

719 number of violated time windows as the subgradient advances, we deem the final solution acceptable  
720 from an operational point of view. In the third case, the optimal solution obtained through the market  
721 mechanism is illustrated in more detail (section 6.4). We conclude with a greedy algorithm to derive  
722 a feasible solution when the duality gap is not equal to zero (section 6.5). Appendix E reports some  
723 additional computational experiments performed on data instances of various sizes.

### 724 6.1. Subgradient convergence - Regulations LBSAU04 and LBSCU04

725 First of all, we consider two regulations, LBSAU04 and LBSCU04, affecting two collapsed sectors in  
726 Bulgaria, that were both limiting the rate to 40 flights per hour due to adverse weather, the first from  
727 13:00 to 14:31 and the second from 13:00 to 16:15. We take as  $\mathcal{F}$  the set of all flights affected by at least  
728 one of the two regulations, and  $\mathcal{L}$  the set of time windows on the two regulations. The set  $\mathcal{F}$  comprises  
729 a total of 111 flights, of which 15 flights were affected by both regulations. The cost of the initial FPFs  
730 allocation is € 960.20. We verified that the duality gap for this instance is zero, and the cost of the TW  
731 allocation (5) is € 263.36 leading to 72.6% cost savings.

732 Figure 3 shows with a blue line the decrease in the Lagrangian function in the first 100 iterations of  
733 the subgradient algorithm applied to such data instance, using stepsize (45). After 100 iterations, the  
734 objective value reaches 100.83% of its minimum value (the pink dotted line), and the prices are still not  
735 exactly at their equilibrium. The algorithm does not converge to an optimal solution of problem (IP)  
736 even after 300 iterations.

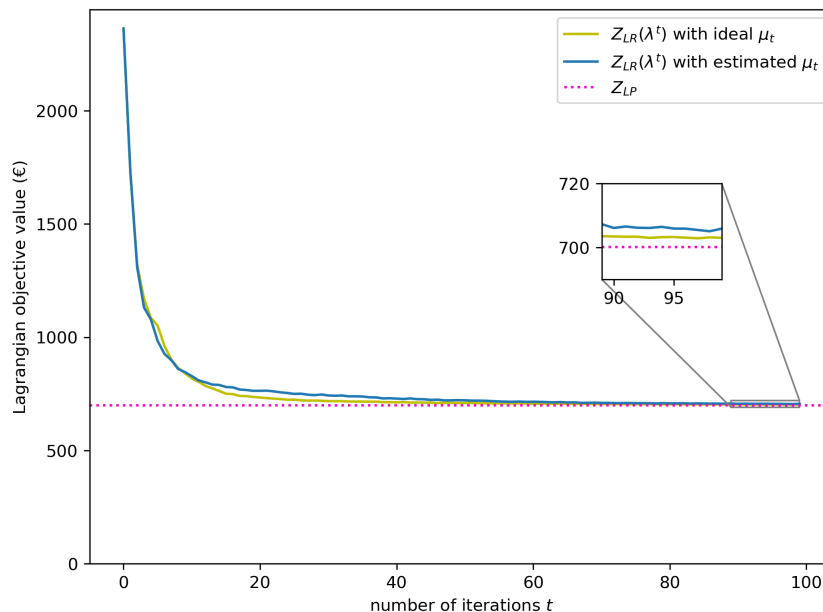


Figure 3: Lagrangian objective value  $Z_{LR}(\lambda^t)$  vs number of iterations  $t$  (with zoom over the last 10 iterations)

737 This behaviour is not caused by the approximation we did by employing the lower bound in the  
738 stepsize formula. As a comparison, we report in the same plot (Figure 3) the result when we run the  
739 subgradient algorithm using the ideal stepsize (22), pretending that costs are known (yellow line). The  
740 convergence profile is very similar. In this case also, convergence to an optimal solution of (IP) does not  
741 happen, even if the final value is slightly lower, 100.42% of the minimum.

742 We found that this is a general trend on other data instances. Using the ideal formula (22) for the  
743 stepsize, the subgradient algorithm rarely converges to a capacity-compliant solution within a reasonable  
744 number of iterations, because prices converge too slowly.

745 In instances for which the duality gap is zero, the subgradient algorithm always converges as discussed  
 746 in Section 4.1.1, at least asymptotically if the ideal stepsize is used.

747 Notice that we used the highest value possible for  $\epsilon_t$  that guarantees convergence, i.e.  $\epsilon_t = 2$ . If we use  
 748 a higher value, on some instances a faster convergence can be achieved, but on some others the objective  
 749 value diverges. With (45) we used  $\epsilon_0 = 3$  to compensate for the fact that  $RES^t$  is an underestimate of  
 750 the true residual.

751 When we use the heuristic formula (46) on our example instance (Figure 4) the algorithm finds  
 752 an optimal solution of (IP) at iteration 83 and terminates. We often achieved finite termination at  
 753 optimality on other small-size instances (two regulations and comparable number of flights) with the  
 754 heuristic formula.

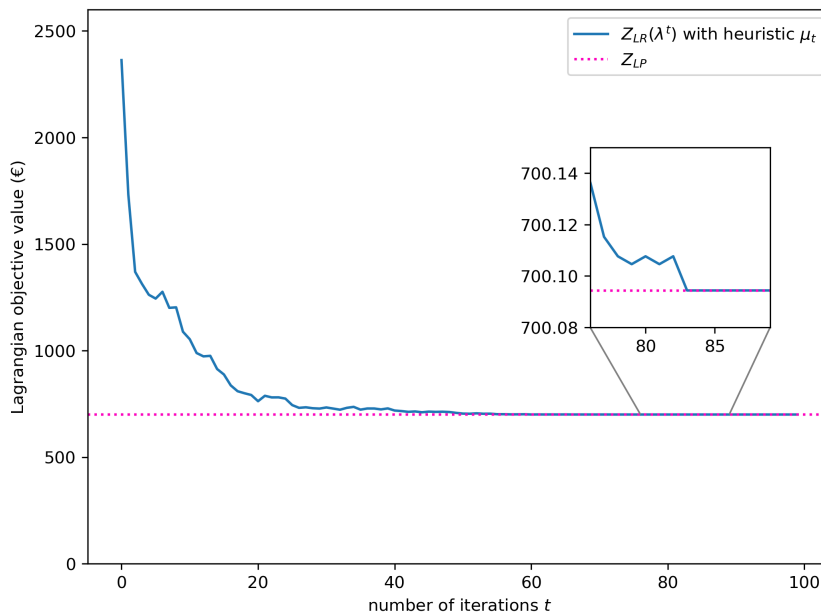


Figure 4: Lagrangian objective value  $Z_{LR}(\lambda^t)$  vs number of iterations  $t$  (with zoom where finite convergence is attained)

755 Figure 5 shows the true value of the residual  $Z_{LR}(\lambda^t) - Z_{LP}$  together with its underestimate  $RES^t$ .  
 756 It is evident that this underestimate is able to reproduce the trend in the real residual. When the real  
 757 residual increases, the underestimate increases too and when the real residual decreases, the underes-  
 758 timate decreases, even if the magnitude of the two is quite different. This provides justification to the  
 759 empirical formula (46), as the underestimate is able to correctly capture when the real objective function  
 760 fails to improve for  $n$  iterations.

761 Figure 6 shows the stepsize sequence obtained when we run the subgradient algorithm with the ideal  
 762 stepsize rule (22), and the stepsize sequence obtained when we use the heuristic rule (46). The heuristic  
 763 stepsize tends to be higher, and we believe that this is the reason of the success of this formula: if the  
 764 magnitude of the step is higher, prices  $\lambda^t$  tend to converge faster, provided that they converge at all. Of  
 765 course, the drawback is that convergence is not guaranteed, so this represents a more aggressive strategy  
 766 for scheduling the stepsize than (22), or actually its version (45) in the case of unknown costs, but less  
 767 robust.

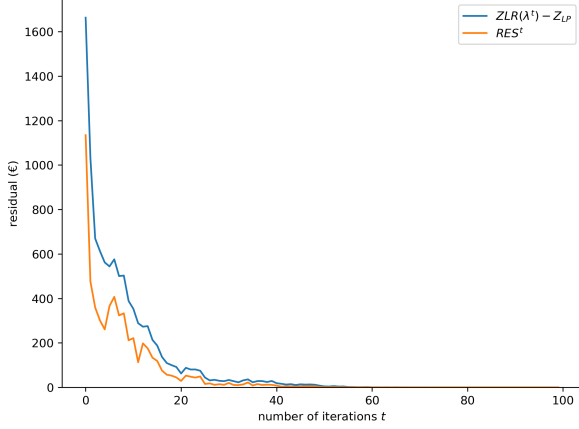


Figure 5: Goodness of the lower bound on the residual

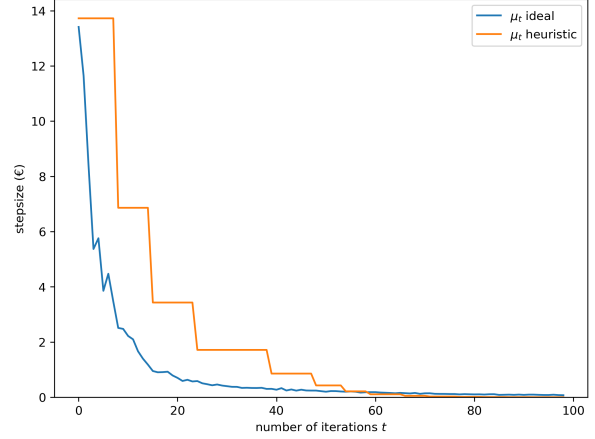


Figure 6: Comparison between stepsize sequences

768 6.2. Weakly budget balanced solution - Regulations LOVS04N and LOWB304A

769 We present an example that shows that the subgradient algorithm finds a capacity-compliant solution  
 770 that is also weakly budget balanced, even if it does not satisfy the complementary slackness conditions.

771 The example is relative to two interacting regulations, LOVS04N and LOWB304A, and a total of  
 772 145 flights affected by at least one of them. We verified that the duality gap for this instance is zero.

773 Figure 7 displays the converge profile on this instance, with a zoom on the last iterations to show that  
 774 convergence is not attained at the minimum of the Lagrangian function, but at a slightly higher value.  
 775 Nonetheless, at iteration 100 the solution of the Lagrangian problem turns out to be capacity-compliant,  
 776 and also weakly budget balanced, even if it does not satisfy complementary slackness. Although the  
 777 solution is not optimal, the subgradient algorithm may be stopped, as the resulting market mechanism  
 778 implied by the current solution satisfies the desired properties.

779 We remark that we can assess the degree to which this near-optimal solution departs from optimality.  
 780 Specifically, we have that  $Z_{IP} - \sum_{f \in \mathcal{F}} V(f, q_f^{*t}) \leq \lambda^t \cdot SG^t$  (Geoffrion, 1974).

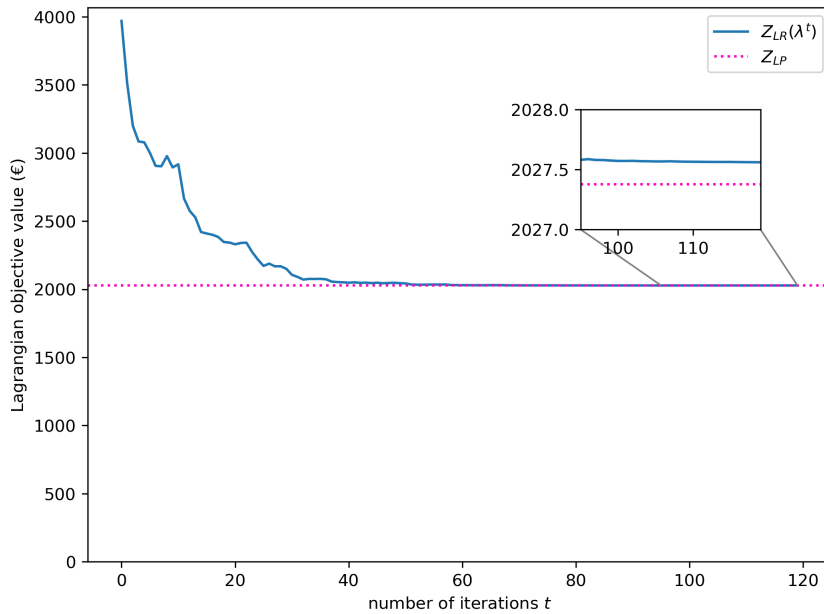


Figure 7: Convergence profile (with detail of the last iterations)

781 6.3. Capacity constraint violation - Regulations LHSUH04A and LONE3504

782 We introduce an example that shows that when the subgradient algorithm does not converge to a  
 783 solution which respects the capacity constraint, often the violation of the capacity constraint is small.  
 784 We consider the regulations LHSUH04A and LONE3504 which affect a total of 233 flights. Figure 8  
 785 shows the convergence profile for our third example instance. The Lagrangian objective value reaches  
 786 100.59% of its minimum after 150 iterations.

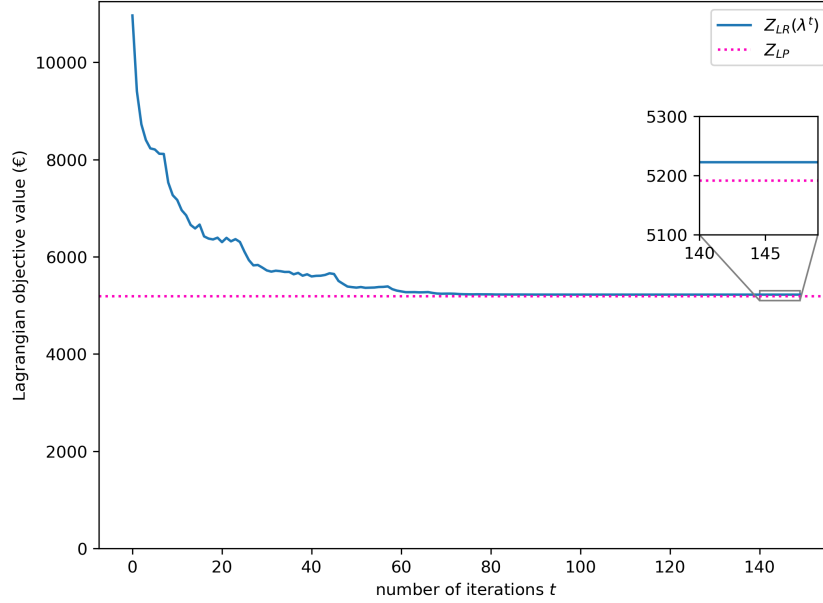


Figure 8: Convergence profile

787 As we discussed in Section 4.1, due to the way the subgradient algorithm is designed, it tends to  
 788 reduce capacity violations during the course of iterations. A step of the subgradient algorithm tends to  
 789 raise the price of time windows for which the demand exceeds the capacity, so that at the next iteration  
 790 the demand will be lower.

791 More quantitatively, let us define the *total overload* of a time window allocation as the total number  
 792 of flights exceeding the capacity of time windows (i.e. 1 flight per time window). Recall that the number  
 793 of flights whose demanded bundle at iteration  $t$  contains time window  $k$  is  $1 - SG_k^t$ . Then, at iteration  
 794  $t$ , the overload  $OL_k^t$  of time window  $k$  is given by  $OL_k^t = \max(0, -SG_k^t)$  and the total overload is given  
 795 by  $\sum_{k \in \mathcal{L}} OL_k^t$ .

796 Figure 9 reveals that the total overload indeed tends to decrease during iterations. If the subgradient  
 797 algorithm would converge to an optimal solution, then the total overload would be zero. At the same  
 798 time, as shown in Figure 10, the surplus  $\sum_{f \in \mathcal{F}} (p^t(q_f^t) - p^t(a_f))$  tends to increase, and after 60 iterations  
 799 it rises above zero.

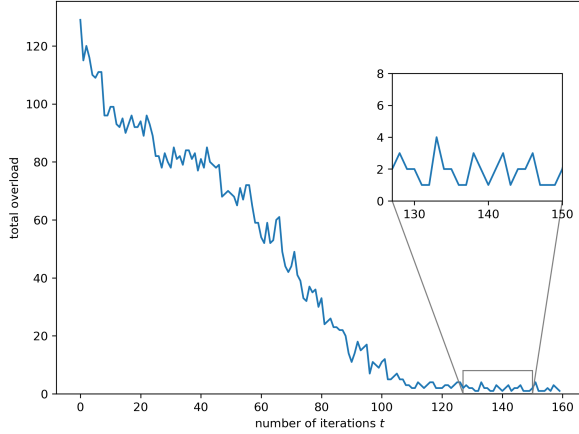


Figure 9: Total overload

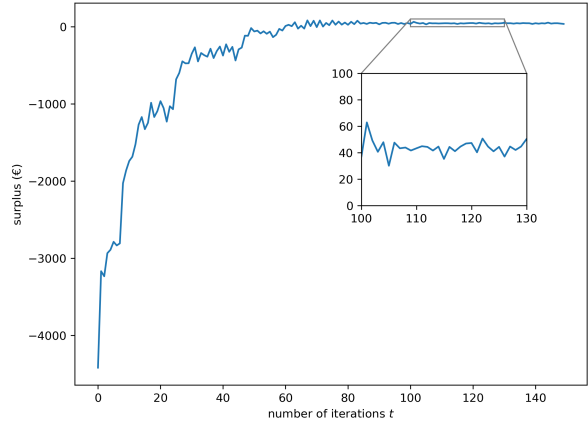


Figure 10: Surplus

800 At iteration  $t = 131$ , there is only one flight in excess with respect to the capacity, i.e. the total  
 801 overload is 1, and the surplus is positive, in particular it amounts to 44.57 €. Although one flight  
 802 could not be appropriately accommodated by the algorithm, in practice it might happen that the ATFM  
 803 controllers and/or the airlines could re-allocate such flight in cost-efficient manner. Therefore, even with  
 804 this small capacity violation, we can be content with this solution.

805 To sum up what we discussed in this section and in Section 4.1.1, these are the factors that prevent  
 806 convergence of the subgradient algorithm to an optimal solution of our allocation problem:

- 807 1. The duality gap may be non-zero, in which case the prices which solve the Lagrangian dual do not  
 808 support the optimal allocation.
- 809 2. There may be multiple solutions of the Lagrangian relaxation subproblem, so even when the duality  
 810 gap is zero and the prices have converged exactly, the subgradient algorithm may not find the  
 811 optimal allocation.
- 812 3. Even if costs were known and the ideal stepsize sequence was used, finite convergence would not  
 813 be guaranteed, and asymptotic convergence does not yield the solution to the allocation problem.
- 814 4. By using an heuristic stepsize rule, in not all cases finite convergence is attained.

815 When the subgradient algorithm stops without converging to the optimal solution, two situations  
 816 can arise. Either the subgradient algorithm solution provides a set of bundles that do not cause slot  
 817 overloads (i.e., no time windows are assigned to more than one flight), or conversely, some slot overload  
 818 does occur (i.e., some time windows are assigned to more than one flight). In the former case, flights may  
 819 decide to accept the proposed solution if it is weakly budget balanced. In the latter case, the presence  
 820 of slot overloads can be handled with the heuristic presented in Section 6.5.

821 We also note, as we have already pointed out, that it is not uncommon in operations to accept  
 822 some slot overloads, i.e., ~~more than one flight in the same time window,~~ are accepted **two flights in the**  
 823 **same sequence time window are often accepted in a sector**, especially if there is a nearby empty slot,  
 824 typically in the range between -20 min and +60 min, that can compensate for the overload. Therefore,  
 825 the acceptability of this type of “imperfect” solution may be worth further investigation in the future.

#### 826 6.4. Market mechanism solution - Regulations ME1204 and MKK04

827 Here we introduce an example on an instance of smaller size (in terms of number of flights), for which  
 828 the space limitation of the paper allows us to report the solution.



829 The interested regulations are ME1204 and MKK04, affecting two en-route sectors near Marseille,  
830 France. The regulation reason for both was ATC Staffing. Regulation MKK04 was active from 11:40 to  
831 13:00 with a capacity of 38 flights/hour, and regulation ME1204 was active from 12:00 to 13:40 with a  
832 capacity of 30 flights/hour. There were 39 flights subject to regulation ME1204 and 40 flights subject to  
833 MKK04, of which 15 to both of them, for a total of 64 flights. Regulation ME1204 has 50 time windows  
834 and MKK04 has 51 time windows. At first sight, it may seem weird that the number of flights subject to  
835 a regulation is smaller than the number of TWs available. But the point is that, if no delay was assigned  
836 to flights, some time windows would have more than one flight passing through them, and some other  
837 time windows would have no flights at all: the purpose of a regulation is to smooth the traffic over the  
838 regulation period.

839 With the subgradient algorithm an optimal solution is found after only 37 iterations. The total delay  
840 under the FPFS allocation is 105 minutes and the total cost of delay is 1159.90€. Under the optimal  
841 allocation the total delay is slightly higher, 106 minutes, but the cost is almost halved, 619.72€. The  
842 surplus from the market mechanism is 7.26€. The sum of profits (utility variations) of all flights is thus  
843  $\sum_{f \in \mathcal{F}} \Delta u(f) = \sum_{f \in \mathcal{F}} (V(f, q_f^*) - p(q_f^*) + p(a_f)) = 1159.90\text{€} - 619.72\text{€} - 7.26\text{€} = 532.92\text{€}$  .

844 It is interesting to look closely at the optimal solution. Table 2 lists all the monetary transactions  
845 between flights and the central authority (CA) prescribed by the market mechanism. The first column  
846 is the TW being exchanged, the second column is the flight selling the TW (releasing the TW from its  
847 FPFS allocation), the third column is the flight buying the TW (taking up the TW under the optimal  
848 allocation), and the fourth column is the payment associated with the TW exchange, i.e. the price of the  
849 TW (see Section 3.3). Time windows not appearing in the table either are not assigned under the FPFS  
850 policy nor under the optimal policy, or they are assigned to the same flight in both policies (we omitted  
851 virtual transactions from a flight to itself from the table). Out of the total of 64 flights, 24 flights were  
852 allocated with the same time windows under both FPFS and optimal policy. These are the flights who  
853 are willing to participate in the process but for whom it is most convenient to keep the FPFS bundle.

854 As an example, consider the two rows of the table involving time windows r1 k48 and r1 k49. Flights  
855 f28 and f54 exchange their FPFS TWs; f28 increases its delay and thus receives a net amount of 23.12€  
856 - 10.8€ = 12.32€ from f54 as a compensation. In many cases the transactions occur between a pair  
857 of flights swapping a time window, as in the example, but in other cases they consist in more complex  
858 trading cycles involving three or more flights.

859 Most trades occur between flights, and only 5 trades occur between a flight and the central authority  
860 (see again cases (ii) and (iii) in Section 3.3). Of these, all are 0€ except one in which flight f63 pays 7.26€  
861 to the central authority for TW r1 k18 and this represents the surplus of the market mechanism. In the  
862 last case, we are in the presence of an airline that is willing to pay for a currently free TW. In such a  
863 situation, the central authority may decide to allocate it free of charge, so that in practice the exchange  
864 would be fully budget balanced. However, a similar policy should be agreed upon with all airlines in  
865 advance. In fact, reducing the price paid by f63 for TW r1 k18 from 7.26€ to 0.00€ may be unfair, since  
866 other flights may then prefer this TW at zero price to their allocated TW, and (19) would not hold.

867 We remark that some TW exchanges or some central authority TW allocations may naturally occur  
868 with price equal to 0€. This is always the case when a flight sells a TW to the central authority, due to  
869 the complementary slackness condition. It can also happen when a flight exchanges a pair of slots with  
870 another flight. For instance, considering Table 2 again, f18 sells its FPFS time window r2 k5 at 0€ to  
871 f19 so that this f19 can sell r2 k4 to f18 and allows it to decrease its delay. In this type of TW exchange,  
872 and in general in circular TW exchanges, the difference in TW prices may be more important than the  
873 price of each individual TW, especially if no other flight is interested in the TWs being considered. As  
874 another example, the circular exchange of TWs r2 k45, k46, and k47 between f3, CA, and f23 at 0€ is  
875 justified even if f3 gets a TW with a greater delay. It allows f3 to be compensated in regulation r1, where

876 its profit is positive because it receives compensation of 24.03€ for the increase in delay.

TW	seller	buyer	payment	TW	seller	buyer	payment
r1 k1	f33	f48	22.81€	r2 k10	f33	f48	46.51€
r1 k3	f48	f11	0.00€	r2 k11	f24	f2	39.56€
r1 k4	f24	CA	0.00€	r2 k12	f48	f10	21.61€
r1 k5	f29	f24	2.70€	r2 k13	f2	f24	10.80€
r1 k6	f11	f29	0.00€	r2 k14	f43	f34	5.40€
r1 k18	CA	f63	7.26€	r2 k15	f22	f43	1.01€
r1 k21	f63	f13	0.00€	r2 k16	f34	f22	0.34€
r1 k22	f13	CA	0.00€	r2 k24	f60	f12	143.94€
r1 k23	f16	f23	10.80€	r2 k25	f12	f60	104.63€
r1 k24	f23	f16	0.00€	r2 k28	f36	f44	30.51€
r1 k30	f3	f14	24.03€	r2 k31	f15	f17	17.53€
r1 k31	f14	f59	10.80€	r2 k32	f44	f63	21.27€
r1 k32	f59	f3	0.00€	r2 k33	f17	f36	4.05€
r1 k37	f41	f27	12.65€	r2 k34	f63	f15	2.70€
r1 k38	f27	f38	10.75€	r2 k35	f16	f20	2.03€
r1 k39	f38	f41	0.00€	r2 k36	f20	f52	13.94€
r1 k44	f62	f26	8.99€	r2 k37	f52	f49	2.38€
r1 k45	f26	f5	7.27€	r2 k38	f49	f16	0.68€
r1 k46	f5	f62	2.70€	r2 k45	f3	f23	0.00€
r1 k48	f28	f54	23.12€	r2 k46	f23	CA	0.00€
r1 k49	f54	f28	10.80€	r2 k47	CA	f3	0.00€
r2 k4	f19	f18	5.40€	r2 k48	f50	f61	44.34€
r2 k5	f18	f19	0.00€	r2 k49	f61	f50	22.53€
r2 k7	f10	f33	76.36€	r2 k50	f21	f1	13.59€

Table 2: Transactions (in the first column, “r1” stands for ME1204, “r2” stands for MKK04; “k1” is the first TW, “k2” is the second etc.)

877 Finally, we show how strict are the bounds on costs obtained by the central authority and used to  
878 compute the stepsize. Figure 11 shows a histogram of the ratios  $\widetilde{LB}^t(f, q)/C(f, q)$  for the last iteration  
879  $t = 37$  for all bundles  $q \in Q_f, f \in \mathcal{F}$ . The bounds  $\widetilde{LB}^t(f, q)$  are computed as in problem (32). For 96%  
880 of the bundles, the lower bound is less than 90% of the true cost value. Figure 12 shows a histogram of  
881  $C(f, q)/\widetilde{UB}^t(f, q)$  for  $t = 37$ . The first bin of the histogram highlights that for 86% of the bundles no  
882 upper bound can be obtained (i.e. problem (32) is unbounded). This means that in practice the cost  
883 elicitation procedure described in Section 4.2.1 does not pose a privacy risk for the airlines.

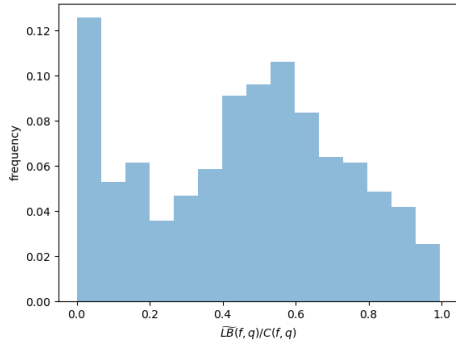


Figure 11: Histogram of the ratio between the lower bound on the cost and the true cost

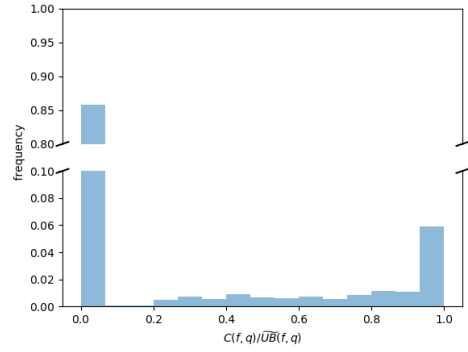


Figure 12: Histogram of the ratio between the true cost and the upper bound on the cost (broken y axis)

884 Appendix E.1 reports some additional computational experiments performed on real instances of  
 885 different sizes with the duality gap equal to zero.

### 886 6.5. Resolution of duality gaps

887 The duality gap was always zero in all the previous examples. However, our experiments confirm the  
 888 expectations that the percentage of problem instances for which the duality gap is zero decreases as the  
 889 instance size (in terms of number of flights and regulations) increases. Here, we discuss how to handle  
 890 these situations, and also the cases where the subgradient algorithm returns a solution that provides  
 891 bundles that cause some slot overloads.

892 A straightforward way to find a feasible solution is to allow only a subset of the flights to exchange  
 893 time windows, while the rest of the flights will maintain their FPFS allocation. We run the subgradient  
 894 algorithm until the objective value is close to its minimum. We consider the time windows for which  
 895 the overload is  $OL_k^t > 0$ . For each of these, we remove from the market mechanism one of the  $OL_k^t$   
 896 flights demanding that time window at time  $t$ , and assign the FPFS bundle to them. This means that  
 897 the size of the set  $\mathcal{F}$  on which the optimisation is performed is reduced. The time windows belonging to  
 898 these FPFS bundles are removed from the set  $\mathcal{K}$  of time windows available for exchange, meaning that  
 899 the feasible bundles of all flights in  $\mathcal{F}$  are filtered from these. Then, the subgradient algorithm is run  
 900 again on this reduced instance, with the hope that the duality gap will be now zero. In the case it is,  
 901 the feasible solution of the reduced optimisation problem is implemented. In the case the duality gap is  
 902 still different from zero, the above procedure of constructing a smaller instance is repeated one or more  
 903 times. This procedure obviously guarantees to terminate with a feasible solution, since in the limit all  
 904 flights are removed from  $\mathcal{F}$  and the FPFS allocation for all flights is implemented. In practice, we found  
 905 that just one iteration is often sufficient.

906 As an example, we used an instance with 5 regulations and 832 flights, depicted in Figure 13 as a  
 907 graph. A node corresponds to a regulation in  $\mathcal{R}$ , and an edge is drawn between every pair of regulations  
 908 which are connected by at least one flight, in the sense that the flight crosses the two regulations  
 909 consecutively. The edge weight represents the number of connections. The delay cost of the initial FPFS  
 910 allocation is equal to € 24364.04 and the savings from the TW allocation (5) are equal to 82.9%. The  
 911 duality gap for this instance is 0.14.

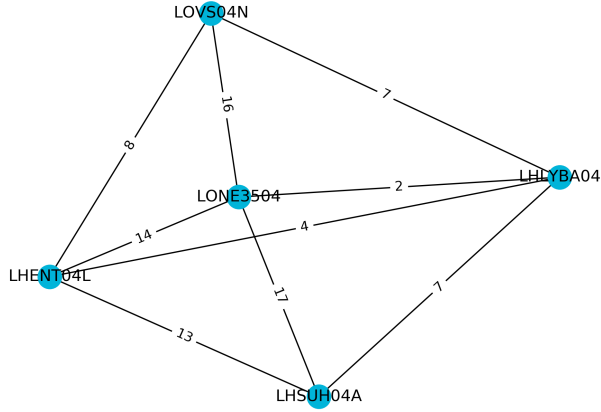


Figure 13: Instance structure

912 For such large instance, it is necessary to decrease the parameter  $\gamma$  appearing in equation (46),  
 913 because convergence is expected to be slower with respect to the four cases encountered before. We set  
 914  $\gamma = 1.2$ . After 371 subgradient iterations on the entire instance, the objective function reaches 100.0002%  
 915 of its minimum value and there are only 4 overloaded time windows. At this point, after removing the 4  
 916 flights in excess with respect to the capacity, the duality gap becomes zero. Restarting the subgradient  
 917 algorithm, an optimal solution is obtained after 410 iterations, with an optimal cost of € 4184.67. By  
 918 adding the cost of the FPFS bundles of the 4 removed flights, we obtain the cost of the feasible solution  
 919 for the entire instance, € 4184.67 + € 6.79 = € 4191.46. This cost is very close to the optimal cost for  
 920 the entire instance, € 4170.23. In other words, the value of this feasible solution is only 21.23€ lower  
 921 than the value of the optimal solution. It is also worth noting that the prices obtained are close to the  
 922 optimal prices. More precisely, for 70% of the time windows the price is less than 10% away from the  
 923 optimal price. The maximum price is 179.81€, and 25% of the time windows have prices equal to zero.

924 Figure 14 shows a histogram of the non-zero prices.

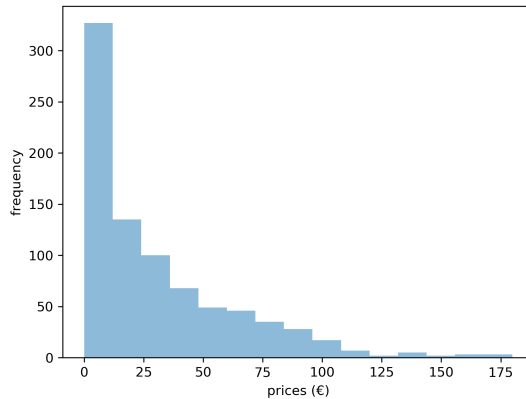


Figure 14: Histogram of non-zero prices

925 Appendix E.2 reports other computational experiments performed on real instances of different sizes  
 926 with the duality gap different zero.

927 *6.6. Concluding remarks on computational experiments*

928 Summing up, the five examples introduced in this section provide some guidelines on how to deal  
 929 with our problem in practice, when it is not known if we are dealing with zero dual-gap instances.

930 When the subgradient algorithm is stopped three situations may occur. If we find a feasible solution  
931 that satisfies the complementary slackness conditions, we are in presence of a zero dual-gap instance and  
932 the algorithm has individuated a Walsarian equilibrium. If the solution does not satisfy the complemen-  
933 tary slackness conditions but it is feasible for (*IP*), this solution is capacity compliant and individual  
934 rational, but may or may not be weakly budget balanced (see Section 6.2 for a weakly budget balanced  
935 instance). If the solution is not feasible for (*IP*) the heuristic proposed in Section 6.5 can be applied.

936 Table 3 summarises the properties of the optimal solution (“opt. sol.”) compared to the FPFS  
937 solution in the four cases with two regulations presented from Section 6.1 to Section 6.4, respectively.  
938 The total delay is not the sum of the two regulations’ delay because the delay of flights passing through  
939 both regulations does not have to be double counted, and similarly for the number of flights and the  
940 cost. We notice that cost savings are always significant (from 33% to 85%), despite sometimes a small  
941 increase in the delay is experienced. The table also reports the number of flights delayed beyond the  
942 upper bound of each regulation period (“n° flights out of reg.”), both in the FPFS and in the optimal  
943 allocation. These are flights occupying a dummy TW. Since their number, if any, is always very low, the  
944 presence of these TWs is not expected to pose problems from an operational point of view. Similarly  
945 to capacity violations addressed in Section 6.3, in practice it might happen that the ATFM controllers  
946 and/or the airlines could re-allocate such flights in a cost-efficient manner.

		section 6.1	section 6.2	section 6.3	section 6.4
		LBSAU04, LBSCU04	LOVS04N, LOWB304A	LHSUH04A, LONE3504	ME1204, MKK04
first regulation	n° flights	39	60	159	39
	cost FPFS	€ 319.82	€ 1,783.97	€ 5,421.41	€ 713.04
	cost opt. sol.	€ 121.13	€ 340.64	€ 1,005.92	€ 477.66
	<b>% of change opt.sol. vs. FPFS</b>	<b>-62%</b>	<b>-81%</b>	<b>-81%</b>	<b>-33%</b>
	delay FPFS	23 min	171 min	554 min	66 min
	delay opt. sol.	27 min	172 min	556 min	64 min
	n° flights out of reg. in FPFS	0	0	2	1
	n° flights out of reg. in opt. sol.	0	0	1	1
second regulation	n° flights	87	112	116	40
	cost FPFS	€ 746.96	€ 2,027.90	€ 1,755.64	€ 1,020.92
	cost opt. sol.	€ 236.26	€ 426.82	€ 264.08	€ 564.30
	<b>% of change opt.sol. vs. FPFS</b>	<b>-68%</b>	<b>-79%</b>	<b>-85%</b>	<b>-45%</b>
	delay FPFS	84 min	192 min	172 min	87 min
	delay opt. sol.	100 min	162 min	189 min	92 min
	n° flights out of reg. in FPFS	1	1	0	1
	n° flights out of reg. in opt. sol.	1	0	0	1
both regulations	n° flights	111	145	233	64
	cost FPFS	€ 960.20	€ 2,689.30	€ 6,328.80	€ 1,159.90
	cost opt. sol.	€ 263.36	€ 661.93	€ 1,121.86	€ 619.72
	<b>% of change opt.sol. vs. FPFS</b>	<b>-73%</b>	<b>-75%</b>	<b>-82%</b>	<b>-47%</b>
	delay FPFS	100 min	268 min	651 min	105 min
	delay opt. sol.	109 min	280 min	666 min	106 min

Table 3: Number of flights, cost and delay of the FPFS solution and the optimal solution, for the two single regulations and in total

## 947 7. Conclusions and future perspectives

948 In this paper, we propose a market-based mechanism for the allocation of time windows in case of  
949 multiple interacting ATFM regulations. We show that significant delay cost reductions are possible for  
950 airlines with respect to the First Planned First Served allocation policy currently adopted in Europe.

951 This market mechanism is allocative efficient, individual rational and weakly budget balanced. It is  
952 based on the Lagrangian relaxation of an integer optimisation problem that can be implemented in a  
953 distributed way with the subgradient method. We have successfully tested the mechanism on real data  
954 instances and discussed possible problems that can arise in convergence of the subgradient method. In  
955 particular, the choice of stepsize for the subgradient method is a delicate matter, which requires to find  
956 a compromise between fast convergence and “robust” convergence (i.e. convergence in all instances).

957 It should be noted that optimised hardware can partially help to resolve this trade-off, but the  
958 inevitable uncertainty that plagues cost values makes it questionable to spend excessive computational  
959 time on finding a solution whose value is approximated anyway.

960 We have shown that convergence to an optimal solution, or even just a feasible solution, is not always  
961 possible. A possible future development would be to try to design a Lagrangian heuristic (Fisher, 2004) to  
962 slightly modify nearly feasible Lagrangian solutions to satisfy the capacity constraint while maintaining  
963 individual rationality and weak budget balance.

964 Another possibility for future experiments could be to leverage the fact that delay costs are not  
965 completely unknown and that recent advances in predicting rerouting costs (Khan et al., 2021) provide  
966 reliable thresholds for airlines to assess whether the acceptance of the delay is economically viable. For  
967 example, before running the subgradient method, to set the stepsize sequence we could initialise prices  
968 of time windows with the optimal dual prices of the allocation problem solved with the estimated costs  
969 available by the central authority. This would facilitate and speed up convergence towards optimal  
970 solutions.

971 A challenging perspective would be to try to apply the model on a large-scale instance, possibly a  
972 whole day of air traffic data. The difficulty is that the duality gap for such large instance is probably non-  
973 zero. Also, this would require to find another rule for the stepsize, because solving a linear optimisation  
974 problem at each iteration would be too computationally expensive.

## 975 References

- 976 Barnhart, C., Bertsimas, D., Caramanis, C., Fearing, D., 2012. Equitable and efficient coordination in traffic flow manage-  
977 ment. *Transportation science* 46, 262–280.
- 978 Berechet, I., Debouck, F., Castelli, L., Ranieri, A., Rihacek, C., 2009. A target windows model for managing 4-d trajectory-  
979 based operations. *AIAA/IEEE Digital Avionics Systems Conference - Proceedings* , 3.D.21–3.D.29.
- 980 Bikhchandani, S., Mamer, J.W., 1997. Competitive equilibrium in an exchange economy with indivisibilities. *Journal of*  
981 *economic theory* 74, 385–413.
- 982 Bolić, T., Castelli, L., Corolli, L., Rigonat, D., 2017. Reducing atfm delays through strategic flight planning. *Transportation*  
983 *Research Part E: Logistics and Transportation Review* 98, 42–59.
- 984 Bolić, T., Castelli, L., Corolli, L., Scaini, G., 2021a. Flexibility in strategic flight planning. *Transportation Research Part*  
985 *E: Logistics and Transportation Review* 154, 102450.
- 986 Bolić, T., Castelli, L., Scaini, G., Frau, G., Guidi, S., 2021b. Flight flexibility in strategic traffic planning: visualisation  
987 and mitigation use case. *CEAS Aeronautical Journal* 12, 847–862.
- 988 Castelli, L., Corolli, L., Lulli, G., 2011a. Critical flights detected with time windows. *Transportation research record* 2214,  
989 103–110.
- 990 Castelli, L., Pesenti, R., Ranieri, A., 2011b. The design of a market mechanism to allocate air traffic flow management  
991 slots. *Transportation research part C: Emerging technologies* 19, 931–943.
- 992 Castelli, L., Pesenti, R., Ranieri, A., 2011c. Short-term allocation of time windows to flights through a distributed market-  
993 based mechanism. *Journal of Aerospace Operations* 1, 29–40.
- 994 Cook, A., 2016. *European air traffic management: principles, practice, and research*. Routledge.
- 995 Cook, A.J., Tanner, G., 2015. *European airline delay cost reference values*.

996 Cook, A.J., Tanner, G., Anderson, S., 2004. Evaluating the true cost to airlines of one minute of airborne or ground delay.

997 Cook, A.J., Tanner, G., Bolic, T., 2021. D3.2 industry briefing on updates to the european cost of delay.

998 Dalmau, R., 2022. Predicting the likelihood of airspace user rerouting to mitigate air traffic flow management delay.

999 Transportation Research Part C: Emerging Technologies 144, 103869.

1000 Delgado, L., Gurtner, G., Bolić, T., Castelli, L., 2021. Estimating economic severity of Air Traffic Flow Management

1001 regulations. Transportation Research Part C: Emerging Technologies 125, 103054.

1002 Fisher, M.L., 2004. The lagrangian relaxation method for solving integer programming problems. Management Science 50,

1003 1861–1871.

1004 Geoffrion, A.M., 1974. Lagrangean relaxation for integer programming, in: Approaches to integer programming. Springer,

1005 pp. 82–114.

1006 Granberg, T., Polishchuk, V., 2012. Socially optimal allocation of ATM resources via truthful market-based mechanisms.

1007 2nd SESAR Innovation Days, 27-29 November 2012, Braunschweig, Germany.

1008 Han, F., Wong, W.B.L., Gaukrodger, S., 2010. Improving future air traffic punctuality: “pinch-and-pull” target windows.

1009 Aircraft Engineering and Aerospace Technology 82, 207–216.

1010 Khan, W.A., Ma, H.L., Ouyang, X., Mo, D.Y., 2021. Prediction of aircraft trajectory and the associated fuel consumption

1011 using covariance bidirectional extreme learning machines. Transportation Research Part E: Logistics and Transportation

1012 Review 145, 102189.

1013 Krishna, V., 2009. Auction theory. Academic press.

1014 Lawler, E.L., Lenstra, J.K., Rinnooy Kan, A.H.G., 1980. Generating all maximal independent sets: Np-hardness and

1015 polynomial-time algorithms. SIAM Journal on Computing 9, 558–565.

1016 Liu, Y., Liu, Y., Hansen, M., Pozdnukhov, A., Zhang, D., 2019. Using machine learning to analyze air traffic management

1017 actions: Ground delay program case study. Transportation Research Part E: Logistics and Transportation Review 131,

1018 80–95.

1019 Lulli, G., Odoni, A., 2007. The european air traffic flow management problem. Transportation science 41, 431–443.

1020 Margellos, K., Lygeros, J., 2013. Toward 4-D Trajectory Management in Air Traffic Control: A Study Based on Monte

1021 Carlo Simulation and Reachability Analysis. IEEE Transactions on Control Systems Technology 21, 1820–1833.

1022 Mehta, R., Vazirani, V., 2020. An incentive compatible, efficient market for air traffic flow management. Theoretical

1023 Computer Science 818, 41–50.

1024 Myerson, R.B., Satterthwaite, M.A., 1983. Efficient mechanisms for bilateral trading. Journal of economic theory 29,

1025 265–281.

1026 Niarchakou, S., Sfyroeras, M., 2021. ATFCM Operations Manual.

1027 Odoni, A.R., 1987. The flow management problem in air traffic control, in: Flow control of congested networks. Springer,

1028 pp. 269–288.

1029 Performance Review Commission, 2019. Performance Review Report 2019. Technical Report. EUROCONTROL.

1030 Pilon, N., Guichard, L., Cliff, K., 2019. Reducing Impact of Delays using Airspace User-Driven Flight Prioritisation. 9th

1031 SESAR Innovation Days, 2-6 December 2019, Athens, Greece.

1032 Pilon, N., Ruiz, S., Bujor, A., Cook, A., Castelli, L., 2016. Improved flexibility and equity for airspace users during

1033 demand-capacity imbalance: An introduction to the user driven prioritisation process. 6th SESAR Innovation Days,

1034 8-10 November 2016, Delft, The Netherlands.

1035 Ranieri, A., 2010. Combinatorial exchange models for a user-driven air traffic flow management in Europe. Ph.D. thesis.

1036 Università degli studi di Trieste.

1037 Rodríguez-Sanz, Á., Comendador, F.G., Valdés, R.M.A., Pérez-Castán, J.A., García, P.G., Godoy, M.N.G.N., 2019. 4D-

1038 trajectory time windows: definition and uncertainty management. Aircraft Engineering and Aerospace Technology 91,

1039 761–782.

1040 Rodríguez-Sanz, Á., Puchol, C.C., Pérez-Castán, J.A., Comendador, F.G., Valdés, R.M.A., 2020. Practical implementation

1041 of 4D-trajectories in air traffic management: system requirements and time windows monitoring. Aircraft Engineering

1042 and Aerospace Technology 92, 1357–1375.

1043 Rosenthal, E., Eisenstein, E., 2016. A rescheduling and cost allocation mechanism for delayed arrivals. Computers and

1044 Operations Research 66, 20–28.

1045 Ruiz, S., Guichard, L., Pilon, N., Delcourte, K., 2019a. A new air traffic flow management user-driven prioritisation process

1046 for low volume operator in constraint: Simulations and results. Journal of Advanced Transportation 2019.

1047 Ruiz, S., Kadour, H., Choroba, P., 2019b. An innovative safety-neutral slot overloading technique to improve airspace

1048 capacity utilisation, in: 9th SESAR Innovation Days.

1049 Ruiz, S., Kadour, H., Choroba, P., 2019c. A novel air traffic flow management model to optimise network delay, in: The

1050 13th USA/Europe Air Traffic Management Research and Development Seminar, Vienna, Austria.

1051 SESAR, 2019. SESAR Solution PJ07.02 SPR-INTEROP/OSED for V2 - Part I.

1052 Sherali, H.D., Hill, J.M., McCrea, M.V., Trani, A.A., 2011. Integrating slot exchange, safety, capacity, and equity mecha-

1053 nisms within an airspace flow program. Transportation Science 45, 271–284.

1054 Vossen, T., Ball, M., 2006a. Optimization and mediated bartering models for ground delay programs. Naval research



1055 logistics (NRL) 53, 75–90.  
1056 Vossen, T.W., Ball, M.O., 2006b. Slot trading opportunities in collaborative ground delay programs. *Transportation*  
1057 *Science* 40, 29–43.  
1058 Zhang, Q., Le, M., Xu, Y., 2021. Collaborative delay management towards demand-capacity balancing within User Driven  
1059 Prioritisation Process. *Journal of Air Transport Management* 91, 102017.

## 1060 Appendix A Discussion on incentive compatibility

1061 In the paper, we assume the incentive compatibility property is always respected, i.e., all partici-  
1062 pants in the market report their preferences honestly. Some of the consequences that may occur if this  
1063 assumption is violated are discussed below, extending similar considerations already made for the case  
1064 of a single regulation, i.e.,  $|\mathcal{R}| = 1$  (Castelli et al., 2011b).

1065 In the centralised mechanism (Section 3), each flight communicates the value of each bundle to the  
1066 central authority which allocates them to all flights, maximising the overall value. Some airline could  
1067 therefore be tempted to communicate false values to gain an advantage (i.e., declare costs greater than  
1068 the real  $C(f, q)$  in order to receive a better position in the optimal allocation). This possibility is  
1069 however mitigated by the fact that, operating in a competitive environment, an airline would need to  
1070 have perfect knowledge of other participants’ costs in order to be sure that its utility would not decrease  
1071 when cheating.

1072 Another action that could be a consequence of dishonest attitudes is the rejection of the allocated  
1073 bundle because it does not match the desired one. This possibility is mitigated by not requiring anyone  
1074 to participate in the mechanism. Even if the market mechanism is individual rational (each participant  
1075 has a non-negative profit from entering the market), there should be no obligation from an airline to  
1076 participate in it. Exactly as with the UDPP (Pilon et al., 2016), if an airline does not want to participate,  
1077 it remains with the slots allocated through the FPFS. Only those airlines that wish to be in the market  
1078 participate. In our setting, this is possible by including in the set  $F'$  introduced in Section 5.2 (flights  
1079 that are not requested to participate in the market mechanism) also the flights that *do not wish* to  
1080 participate in it. Those who participate are then required to accept the solution provided. Of course,  
1081 an airline that agrees to participate in the centralised mechanism could still provide false cost values to  
1082 the authority. However, this case falls under the one described in the previous paragraph.

1083 Alternatively, applying an iterative procedure similar to the one illustrated in section 6.5 (“The idea  
1084 is to allow only a subset of the flights to exchange time windows, while the rest of the flights will maintain  
1085 their FPFS allocation”), one could also think of a multi-step scheme in which an airline can reject the  
1086 solution proposed by the market mechanism. In the first step, the TW allocation is made to all flights.  
1087 Within a certain instant of time, the airline decides whether to accept or keep the FPFS slot and then  
1088 the allocation is performed again only on those who accepted. Reasons for refusal could be either because  
1089 you have tried to cheat the system or because, in good faith, you have made an incorrect assessment  
1090 of your costs. The flight dispatcher might not accept the market solution because he/she knows from  
1091 experience that FPFS is better. Clearly, this whole process should be regulated (e.g., a maximum number  
1092 of refusals or penalties for refusals could be envisaged) in order to avoid continual attempts by airlines  
1093 to test the system until the desired bundle is obtained, and to give stability to the solution of those who  
1094 do adhere. A detailed design of this scheme is, however, outside the scope of this study and may be the  
1095 subject of future work.

1096 In the distributed case (Section 4), at each iteration the central authority communicates the TW  
1097 prices and each flight identifies the optimal bundle for it at those prices. For example, for flight  $f_1$  the  
1098 optimal bundle contains the TW called  $a_1$  available at price  $p_1$ .  $f_1$  could actually communicate another  
1099 bundle that, for example, contains  $a_2$  instead of  $a_1$  to lower the price of the latter at the next iteration.  
1100 This operation is risky, however, since  $a_1$  could also be requested by another flight  $f_2$  willing to pay  $p_1$

1101 for it, and thus  $f_1$  has to make content with  $a_2$  from which it obtains a lower payoff. As in the case of  
 1102 the centralised mechanism, the existing competition for critical resources makes opportunistic behaviour  
 1103 complex.

## 1104 Appendix B Construction of feasible bundles

1105 Algorithm 1 describes how to generate the set of feasible bundles  $Q_f$  for any flight  $f$ . Bundles are  
 1106 constructed in sequence, from the one having the smallest delay to the one with the largest delay. The  
 1107 first bundle in  $Q_f$  is the bundle whose time windows contain the expected times of entry  $E_f$ . This bundle  
 1108 will have zero delay. Then, the idea is to shift a sequence of time instants  $t$ , initialised with  $E_f$ , towards  
 1109 the right of the discretised timeline and keep track of which time windows contain  $t$  in each element of  
 1110  $R_f$ ; as soon as the time windows change, a new bundle will be appended to  $Q_f$ . Starting from  $t = E_f$   
 1111 and shifting  $t$  towards higher times, you will remain inside the same time windows until you encounter  
 1112 the first upper border of a time window. When an upper bound (or more than one) is encountered, you  
 1113 take the next time window in the slot allocation list of this resource(s), while the other time windows  
 1114 stay the same, and append this new bundle to  $Q_f$ . The delay will be the temporal distance between  
 1115 the lower bound of the new time window and the expected time over the corresponding resource. This  
 1116 procedure is repeated iteratively until either the maximum delay  $MaxDel_f$  is reached, or the end of all  
 1117 slot allocation lists is reached. In the case that  $MaxDel_f$  is reached before all time windows become  
 1118 dummy time windows, the empty bundle corresponding to flight cancellation is added to  $Q_f$ .

---

### Algorithm 1: Construction of feasible bundles

---

**Input:**  $R_f, E_f, \{\hat{L}_r \text{ for } r \in R_f\}, MaxDel_f$

**Output:**  $Q_f$

```

1   $n \leftarrow |R_f|$ ;
2   $t \leftarrow E_f$ ;
3   $q \leftarrow [TW_1, \dots, TW_n]$  where  $TW_i$  is such that  $I_{TW_i} \leq e_i \leq U_{TW_i}$  for  $i = 1, \dots, n$ ;
4   $delay \leftarrow 0$  seconds;
5   $Q_f \leftarrow \emptyset$ ;
6  while  $delay < MaxDel_f$  do
7  |    $d_{q_f} \leftarrow delay$ ;
8  |    $Q_f \leftarrow Q_f \cup q$ ;
1119 9  |   if all  $TW_i \in q$  are dummy then break;
10  |    $interval \leftarrow [U_{TW_1} - t_1, \dots, U_{TW_n} - t_n]$ ;
11  |    $gap \leftarrow \min(interval)$ ;
12  |    $q \leftarrow [TW_i + 1 \text{ if } interval_i = gap \text{ else } TW_i \text{ for } i = 1, \dots, n]$ ;
13  |    $shift \leftarrow gap + 1$  second;
14  |    $t \leftarrow [t_1 + shift, \dots, t_n + shift]$ ;
15  |    $delay \leftarrow delay + shift$ ;
16 end
17 if any  $TW_i \in q$  is not dummy then
18 |    $Q_f \leftarrow Q_f \cup []$ ;
19 end

```

---

## 1120 Appendix C Algorithm for FPFS

1121 This appendix provides an algorithm, adapted from Ranieri (2010), for computing the FPFS bundle  
 1122  $a_f$  for all  $f \in \mathcal{F}$ . Here we will denote  $e_r^f$  the ETO of flight  $f$  in regulation  $r$ . We will consider the set

1123  $Q_f$  as ordered by increasing delay, and with a little abuse of notation we will identify a bundle  $q$  with its  
1124 index in the ordered list  $Q_f$ , for example the most-preferred bundle is  $q = 1$ . We will denote  $TW_r \in q$   
1125 the time window in  $q$  which belongs to regulation  $r$ .

1126 The algorithm begins with variable initialisation at lines 1-9. Variable  $provalloc(f)$  is the tentative  
1127 FPFs allocation for flight  $f$ . During the course of the algorithm, a time window can be assigned to  
1128 multiple flights according to  $provalloc$ , but at the end of the algorithm at most one flight has assigned  
1129 any time window. Variable  $processed(f, r)$  is *True* whenever the time window assigned to  $f$  in regulation  
1130  $r$  is not assigned to another flight whose ETO is smaller.

1131 The algorithm applies the FPFs policy independently on each regulation (lines 11-15). This implies  
1132 that the bundle assigned by the FPFs in one regulation might not respect the FPFs order in another  
1133 regulation, thus the algorithm iteratively adjusts the allocation (lines 16-26) until the FPFs property  
1134 is respected for each flight (line 10) and the capacity constraint is satisfied. At the end of the while  
1135 loop, also the Most Penalizing Regulation rule is satisfied. The second while loop (lines 31-42) checks  
1136 whether some flights can be assigned a bundle with a smaller delay without breaking the FPFs rule and  
1137 the capacity constraint.

---

**Algorithm 2:** FPFS

---

```
1 for  $f \in \mathcal{F}$  do
2    $provalloc(f) \leftarrow None$ ;
3   for  $r \in R_f$  do
4      $processed(f, r) \leftarrow False$ ;
5   end
6 end
7 for  $r \in \mathcal{R}$  do
8    $F_r \leftarrow ordered\_flight\_list(r)$ ;
9 end
10 while  $all\_processed() = False$  do
11   for  $r \in \mathcal{R}$  do
12     for  $f \in F_r$  do
13       if  $provalloc(f) = None$  then
14          $assign\_first\_feasible(f, r, 1)$ ;
15          $processed(f, r) \leftarrow True$ ;
16       else if  $processed(f, r) = False$  then
17         if  $is\_feasible(provalloc(f), f, r) = True$  then
18            $processed(f, r) \leftarrow True$ ;
19         else
20           for  $z \in R_f : z \neq r$  do
21              $processed(f, z) \leftarrow False$ ;
22           end
23            $assign\_first\_feasible(f, r, provalloc(r))$ ;
24            $processed(f, r) \leftarrow True$ ;
25         end
26       end
27     end
28   end
29 end
30  $noimprovement \leftarrow False$ ;
31 while  $noimprovement = False$  do
32    $noimprovement \leftarrow True$ ;
33   for  $f \in \mathcal{F}$  do
34     for  $q \in Q_f : q < provalloc(f)$  do
35       if  $all\_feasible(q, f, r) = True$  then
36          $do\_assign(f, q)$ ;
37          $noimprovement \leftarrow False$ ;
38         break;
39       end
40     end
41   end
42 end
43 for  $f \in \mathcal{F}$  do
44    $a_f \leftarrow provalloc(f)$ ;
45 end
```

1138

1139 The function *ordered\_flight\_list*( $r$ ) returns the list of flights crossing  $r$  ordered by increasing  $e_r^f$ .  
1140 The function *all\_processed*() returns *True* if *processed*( $f, r$ ) = *True* for all  $f \in \mathcal{F}$ ,  $r \in R_f$ .  
1141 The function *all\_feasible*( $q, f, r$ ) returns *True* if *is\_feasible*( $q, f, r$ ) = *True* for all  $r \in R_f$ .  
1142 The function *assign\_first\_feasible*( $f, r, i$ ) assigns to  $f$  the first bundle in  $Q_f$  whose index is at least  
1143  $i$  and such that  $TW_r \in q$  is either not assigned to any other flight, or for all flights  $g$  to which it is  
1144 assigned it holds  $e_r^g > e_r^f$ . In this latter case, we also set *processed*( $g, r$ )  $\leftarrow$  *False*.  
1145 The function *is\_feasible*( $q, f, r$ ) returns *True* if  $TW_r \in q$  for flight  $f$  has not been assigned to any  
1146 other flight.  
1147 The function *do\_assign*( $f, q$ ) assigns bundle  $q$  to flight  $f$ .  
1148 For the sake of efficiency, the five functions described above make use of a data structure which maps  
1149 every time window to the set of flights that are currently assigned to it according to *provalloc*.

## 1150 Appendix D Proof of bounds

### 1151 D.1 Bound on optimal value

1152 Problem (39) is the same of the linear relaxation of problem (5) with the objective function coefficients  
1153  $V(f, q)$  substituted by lower bounds  $LB^t(f, q)$ . The feasible region of (39) is the same as the feasible  
1154 region of the linear relaxation of (5), and the objective function of (39) is everywhere lower than the  
1155 objective function of (5). In fact, from

$$LB^t(f, q) \leq V(f, q) \quad \forall f \in \mathcal{F}, q \in Q_f$$

1156 it follows, since  $x$  is feasible and so  $x(f, q) \geq 0$ ,

$$LB^t(f, q)x(f, q) \leq V(f, q)x(f, q) \quad \forall f \in \mathcal{F}, q \in Q_f$$

1157 and by summing over  $f \in \mathcal{F}$  and  $q \in Q_f$

$$\sum_{f \in \mathcal{F}} \sum_{q \in Q_f} LB^t(f, q)x(f, q) \leq \sum_{f \in \mathcal{F}} \sum_{q \in Q_f} V(f, q)x(f, q)$$

1158 Therefore,  $ZLB^t \leq ZLP$ . Analogously, if  $LB^t(f, q)$  is substituted by an upper bound  $UB^t(f, q)$ , we  
1159 obtain that the optimal value of (39) is an upper bound for the optimal value of the linear relaxation of  
1160 (5).

### 1161 D.2 Non-negativity of a bound

1162 The lower bound  $RES^t$  on  $ZLR(\lambda^t) - ZLP$  is given by

$$RES^t = SG^t \cdot \lambda^t - \max_{x \in \mathcal{S}} \sum_{f \in \mathcal{F}} \sum_{q \in Q_f} (p^t(q) - p^t(q_f^{*t})) x(f, q). \quad (47)$$

1163 If the duality gap  $ZIP - ZLP$  is zero, the maximisation problem appearing in (47) has always an integer  
1164 optimal solution, since its feasible region is the same as the feasible region of the linear relaxation of  
1165 problem (5). Let  $\{q_f^{ot}\}_{f \in \mathcal{F}}$  be the set of bundles corresponding to the optimal solution. Then we can  
1166 write

$$\begin{aligned} RES^t &= \sum_{k \in \mathcal{L}} \lambda_k^t \left( 1 - \sum_{f \in \mathcal{F}} \sum_{q \in Q_f: q \ni k} x^t(f, q) \right) - \sum_{f \in \mathcal{F}} (p^t(q_f^{ot}) - p^t(q_f^{*t})) \\ &= \sum_{k \in \mathcal{L}} \lambda_k^t - \sum_{f \in \mathcal{F}} \sum_{q \in Q_f} \sum_{k \in q} \lambda_k^t x^t(f, q) - \sum_{f \in \mathcal{F}} (p^t(q_f^{ot}) - p^t(q_f^{*t})) \\ &= \sum_{k \in \mathcal{L}} \lambda_k^t - \sum_{f \in \mathcal{F}} p^t(q_f^{*t}) - \sum_{f \in \mathcal{F}} p^t(q_f^{ot}) + \sum_{f \in \mathcal{F}} p^t(q_f^{*t}) \\ &= \sum_{k \in \mathcal{L}} \lambda_k^t - \sum_{f \in \mathcal{F}} p^t(q_f^{ot}) \geq 0 \end{aligned}$$

1167 where the inequality follows from the fact that  $\{q_f^{ot}\}_{f \in \mathcal{F}}$  are capacity-compliant, thus they share no time  
 1168 windows.

## 1169 Appendix E Additional computational results

### 1170 E.1 Instances with zero duality gap

1171 Tables 4 and 5 present some additional computational experiments performed. The table has been  
 1172 split for reasons of space. The first four rows (a, b, c and d) are the four cases already presented in  
 1173 sections 6.1, 6.2, 6.3 and 6.4. The duality gap was zero for all cases in the table. Table 4 contains the  
 1174 following columns: names of the regulations, number of regulations, total number of flights, number of  
 1175 flights subject to at least two of the regulations. Table 5 contains: number of iterations, final overload,  
 1176 whether or not the solution found is optimal, surplus, cost of the FPFS allocation, cost of the optimal  
 1177 allocation, cost of the allocation found (in case it is not optimal). Notice that if the overload is nonzero,  
 1178 the latter cost can be smaller than the optimal cost, since the allocation found is not a proper solution.  
 1179 All these costs are unknown to the central authority. The cost savings are between 47% and 85%, and  
 1180 the cost of the solution found is at most 6% higher than the optimal cost.

	regulations	num. reg.	num. flights	num. flights with $R_f > 1$
a	LBSAU04, LBSCU04	2	111	15
b	LOVS04N, LOWB304A	2	145	27
c	LHSUH04A, LONE3504	2	233	42
d	ME1204, MKK04	2	64	15
e	RMZU04E, RQXU04E	2	143	39
f	EGKKA04, RJS04	2	163	25
g	KCHI104A, LOW3504A	2	259	73
h	EDDLA04, EDWSUD04	2	119	10
i	LHNLMU04, LHWSEN04, LOVSC04	3	82	13
j	EDGN004M, GL67W04, YB3LL04M	3	114	20
k	GL67W04, PDMX04M, YB3LL04M	3	123	25
l	EHYR04M, RESTU04, RG04A	3	170	30
m	KDON1D04, KFFM2404, KWUR1C04	3	221	54
n	K11UFX04, LHENH04, LHENU04	3	275	39
o	EDMBBG04, EDMHAG04, K11UFX04	3	206	25
p	GL12W04, GL5W04, MGY04A, ZM3404	4	363	36
q	KDON104N, KFFM1C04, KFFMC04A	3	414	99

Table 4: Description of the instances, zero duality gap

### 1181 E.2 Instances with nonzero duality gap

1182 Tables 6 and 7 present additional computational experiments performed with the algorithm of Section  
 1183 6.5. In all cases the duality gap was reduced to zero after the first iteration of the algorithm and the  
 1184 optimal solution of the reduced problem (which is a feasible solution of the whole problem) was found  
 1185 in the second iteration. The first row of the table is the case already presented in Section 6.5. The  
 1186 columns of Table 7 are: number of iterations performed on the whole problem, number of iterations  
 1187 on the reduced problem, magnitude of the duality gap, number of flights removed, cost of the FPFS  
 1188 allocation, cost of the optimal allocation of the whole problem, cost of the feasible solution found. The

	num. iter.	overload	is sol. opt.	surplus	FPFS cost	opt. cost	solution cost
a	83	0	true	€ 0.00	€ 960.20	€ 263.36	
b	100	0	false	€ 13.15	€ 2,689.30	€ 661.93	€ 662.93
c	131	1	false	€ 44.57	€ 6,328.80	€ 1,121.86	€ 1,068.50
d	37	0	true	€ 7.26	€ 1,159.90	€ 619.72	
e	141	0	false	€ 11.37	€ 6,559.48	€ 1,021.94	€ 1,070.14
f	122	0	true	€ 0.00	€ 9,537.10	€ 1,823.13	
g	184	1	false	€ 73.12	€ 10,932.82	€ 2,153.40	€ 2,228.41
h	111	1	false	€ 46.27	€ 11,640.81	€ 1,981.35	€ 1,897.21
i	66	0	true	€ 14.82	€ 2,055.24	€ 1,042.56	
j	109	0	true	€ 58.08	€ 3,761.87	€ 843.38	
k	141	0	true	€ 8.89	€ 4,484.10	€ 913.96	
l	138	0	false	€ 95.87	€ 6,375.28	€ 911.90	€ 932.05
m	157	0	false	€ 34.42	€ 8,675.39	€ 1,612.18	€ 1,660.24
n	169	0	false	€ 36.31	€ 21,496.61	€ 3,800.02	€ 4,031.79
o	183	0	true	€ 58.67	€ 13,792.50	€ 2,107.29	
p	191	0	true	€ 0.00	€ 12,195.43	€ 3,964.32	
q	223	2	false	€ 90.36	€ 18,380.43	€ 3,460.63	€ 3,518.02

Table 5: Computational results, zero duality gap

1189 cost of the feasible solution is most often less than 10% more than the optimal cost, and at most 50%  
1190 higher, and the savings with respect to the FPFS solution are between 71% and 89%.

regulations	num. reg.	num. flights	num. flights with $Rf > 1$	
a	LHENT04L, LHLYBA04, LHSUH04A, LONE3504, LOVS04N	5	832	81
b	CBHRE04, EGKKA04, EHYR04M, RJS04	4	345	85
c	MAB04L, MRAEE04L	2	61	13
d	LEBLA04A, MMF04A	2	82	10
e	EKHR04, RMZU04E, RQXU04E	3	165	50
f	EDMBBG04, EDMHAG04, K11UFX04	3	206	25
g	KFFM204A, KWUR04A	2	253	66
h	KFFM2404, KTGO1T04, KWUR04, KWUR2404, LHWSUH04	5	475	120
i	EDGN004M, GL67W04, PDMX04M, YB3EH04M, YB3LL04M	5	426	51
j	CPBDL04, K11UFX04, KHVL1H04, LHENLM04, LOE1504	5	703	80

Table 6: Description of the instances, nonzero duality gap

	num. iter. first round	num. iter. second round	duality gap	num. flights removed	FPFS cost	opt. cost	solution cost
a	371	410	0.14	4	€ 24,364.04	€ 4,170.23	€ 4,191.46
b	387	484	1.66	4	€ 31,779.53	€ 3,396.45	€ 3,499.92
c	83	233	0.06	1	€ 1,145.10	€ 171.72	€ 224.23
d	185	386	0.23	1	€ 1,741.77	€ 286.01	€ 286.14
e	552	366	2.35	1	€ 6,798.12	€ 1,104.81	€ 1,296.86
f	600	370	0.17	4	€ 13,777.47	€ 2,131.83	€ 2,276.11
g	154	204	8.97	6	€ 8,885.98	€ 1,685.85	€ 2,532.98
h	479	505	8.40	4	€ 15,992.62	€ 2,704.83	€ 2,836.05
i	563	341	0.88	6	€ 15,002.05	€ 3,376.16	€ 3,766.67
j	537	442	0.73	3	€ 36,963.43	€ 7,754.63	€ 7,890.24

*Table 7: Computational results, nonzero duality gap*